

$B \rightarrow V_L V_L$ Decays at Next-to-Leading Order in QCD

MATTHÄUS BARTSCH¹, GERHARD BUCHALLA¹ AND CHRISTINA KRAUS^{1,2}

¹Ludwig-Maximilians-Universität München, Fakultät für Physik,
Arnold Sommerfeld Center for Theoretical Physics, D-80333 München, Germany

²Max-Planck-Institut für Quantenoptik,
Hans-Kopfermann-Str. 1, D-85748 Garching, Germany

Abstract

We compute the amplitudes for the two-body decay of B mesons into longitudinally polarized light vector mesons at next-to-leading order in QCD. We give the explicit expressions in QCD factorization for all 34 transitions of a heavy-light B meson into a pair of longitudinal vector mesons ρ , ω , ϕ , K^* within the Standard Model. Decay rates and CP asymmetries are discussed in detail and compared with available data. Exploiting the fact that QCD penguins are systematically smaller for vector mesons in comparison to pseudoscalars in the final state, we investigate several methods to achieve high-precision determinations of CKM parameters and New Physics tests. We propose a method to use V-spin symmetry and data on $\bar{B}_d \rightarrow \bar{K}_L^{*0} K_L^{*0}$ to constrain the penguin contribution in $\bar{B}_d \rightarrow \rho_L^+ \rho_L^-$. CP violation in the latter decay together with a measurement of $\sin 2\beta$ determines the unitarity triangle with high accuracy. We show that CP violation in $\bar{B}_d \rightarrow \rho_L^+ \rho_L^-$ and $\bar{B}_d \rightarrow \psi K_S$ alone implies $|V_{ub}| = (3.54 \pm 0.17) \cdot 10^{-3}$, presently the most accurate determination of this quantity.

1 Introduction

Charmless hadronic B -meson decays provide us with important information on the physics of flavour, within and beyond the Standard Model. After the very successful first generation of B -factory experiments, BaBar and Belle, the interest in this field is re-inforced by the upcoming start of the LHC with the dedicated LHCb experiment [1]. In the longer run the second generation B -factory projects SuperB [2] and SuperKEKB [3] promise excellent future opportunities [4,5], as well as the LHCb upgrade options [1].

In the present paper we investigate in detail the class of hadronic two-body decays of B^- , \bar{B}_d and \bar{B}_s mesons with longitudinally polarized light vector mesons (ρ^\pm , ρ^0 , ω , ϕ , $K^{*\pm}$, \bar{K}^{*0} , K^{*0}) in the final state. These can be computed systematically using QCD factorization in the heavy-quark limit [6,7,8]. In comparison, B decays into vector mesons with transverse polarization are suppressed by powers of Λ_{QCD}/m_b . Their amplitudes do not factorize, as indicated by infrared singularities in convolution integrals, and this introduces a model-dependence in the computation of the related observables [9,10,11]. For this reason we do not include final states with transversely polarized vector mesons in our present analysis, although they raise issues of interest in their own right [9]. Rather, we will pursue the physics of $B \rightarrow V_L V_L$ decays, which comprise 28 calculable channels and 6 annihilation modes within the Standard Model and offer a rich phenomenology by themselves. The various decay modes probe different types of amplitudes, such as tree, QCD and electroweak penguin, or weak annihilation. The large number of channels will allow us to test our understanding of QCD in hadronic B decays and at the same time to extract flavour parameters and search for New Physics effects. An important motivation for the study of final states with two vector mesons is the considerably smaller size of QCD penguin contributions, as compared to the decay into pseudoscalars. This improves our control of QCD effects in several observables of interest for flavour physics. Mixing-induced CP violation in $\bar{B}_d \rightarrow \rho_L^+ \rho_L^-$ is an important example.

Several studies of $B \rightarrow VV$ decays based on factorization in the heavy-quark limit have been made in the literature [9–18]. So far the only comprehensive analysis, including all channels, has been given in [11], where also transverse polarization is discussed. The other articles have addressed various aspects of $B \rightarrow VV$ decays, investigating particular channels, polarization effects and, in part, New Physics contributions.

In this paper we present a detailed analysis of the complete set of $B \rightarrow V_L V_L$ decays within the Standard Model. We work to next-to-leading order (NLO) in QCD, using factorization in the heavy-quark limit. Power corrections to this limit, in particular from weak annihilation, are estimated using a model description [6]. Our presentation includes some additional aspects and several new applications of $B \rightarrow V_L V_L$ transitions. We give detailed analytical expressions for all 34 $B \rightarrow V_L V_L$ decay amplitudes at next-to-leading order. We suggest an alternative treatment of long-distance electromagnetic penguins, which contribute in channels with the neutral vector mesons ρ^0 , ω or ϕ . The effects of ω - ϕ mixing are briefly discussed. We apply the results in new ways to the phenomenology of the unitarity triangle: we use the formulation of [19,20] for the analysis of CP violation in $\bar{B}_d \rightarrow \rho_L^+ \rho_L^-$, we propose an approach to independently constrain the $\bar{B}_d \rightarrow \rho_L^+ \rho_L^-$

penguin with $\bar{B}_d \rightarrow \bar{K}_L^{*0} K_L^{*0}$ and V-spin symmetry, and we extract accurate values of the CKM quantities $\bar{\rho}$, $\bar{\eta}$, γ , α and $|V_{ub}|$.

The paper is organized as follows. Section 2 collects basic ingredients of the calculation, in particular the effective Hamiltonians, form factors, light-cone wave functions and meson projectors. Section 3 presents the NLO results for the $B \rightarrow V_L V_L$ decay amplitudes. Input parameters and experimental results are summarized in section 4. Section 5 contains the phenomenological analysis, with a discussion of branching fractions and CP asymmetries and with precision determinations of the unitarity triangle. A brief comparison with the literature is given in section 6, before we conclude in section 7. Our treatment of long-distance electromagnetic penguins is discussed in the appendix.

2 Preliminaries

The effective weak Hamiltonian for charmless hadronic B decays, without change in strangeness ($\Delta S = 0$), is given by [21]

$$\mathcal{H}_{\text{eff}}^{\Delta S=0} = \frac{G_F}{\sqrt{2}} \sum_{p=u,c} \lambda_p \left(C_1 Q_1^p + C_2 Q_2^p + \sum_{i=3,\dots,10} C_i Q_i + C_{7\gamma} Q_{7\gamma} + C_{8g} Q_{8g} \right) + \text{h.c.} \quad (1)$$

where the elements of the CKM quark-mixing matrix V enter as $\lambda_p = V_{pb}V_{pd}^*$, C_i are Wilson coefficients, and the operators Q_i read

$$\begin{aligned} Q_1^p &= (\bar{p}b)_{V-A}(\bar{d}p)_{V-A}, & Q_2^p &= (\bar{p}_i b_j)_{V-A}(\bar{d}_j p_i)_{V-A}, \\ Q_3 &= (\bar{d}b)_{V-A} \sum_q (\bar{q}q)_{V-A}, & Q_4 &= (\bar{d}_i b_j)_{V-A} \sum_q (\bar{q}_j q_i)_{V-A}, \\ Q_5 &= (\bar{d}b)_{V-A} \sum_q (\bar{q}q)_{V+A}, & Q_6 &= (\bar{d}_i b_j)_{V-A} \sum_q (\bar{q}_j q_i)_{V+A}, \\ Q_7 &= (\bar{d}b)_{V-A} \sum_q \frac{3}{2} e_q (\bar{q}q)_{V+A}, & Q_8 &= (\bar{d}_i b_j)_{V-A} \sum_q \frac{3}{2} e_q (\bar{q}_j q_i)_{V+A}, \\ Q_9 &= (\bar{d}b)_{V-A} \sum_q \frac{3}{2} e_q (\bar{q}q)_{V-A}, & Q_{10} &= (\bar{d}_i b_j)_{V-A} \sum_q \frac{3}{2} e_q (\bar{q}_j q_i)_{V-A}, \\ Q_{7\gamma} &= \frac{e}{8\pi^2} m_b \bar{d} \sigma_{\mu\nu} (1 + \gamma_5) F^{\mu\nu} b, & Q_{8g} &= \frac{g}{8\pi^2} m_b \bar{d} \sigma_{\mu\nu} (1 + \gamma_5) G^{\mu\nu} b \end{aligned} \quad (2)$$

Here i, j are colour indices, e_q are the quark charges, and the sums extend over $q = u, d, s, c, b$. The Wilson coefficients C_i will be taken at next-to-leading order (NLO), using the treatment of electroweak contributions described in detail in [6]. The sign conventions for the electromagnetic and strong coupling correspond to the covariant derivative $D_\mu = \partial_\mu + ieQ_f A_\mu + igT^a A_\mu^a$. With these definitions the coefficients $C_{7\gamma}$, C_{8g} are negative in the Standard Model, which is the convention usually adopted in the literature.

The effective Hamiltonian for charmless decays of B mesons with $\Delta S = 1$ can be obtained from (1) by interchanging d - and s -quark labels. The CKM factors governing these transitions are then $\lambda'_p = V_{pb}V_{ps}^*$.

To obtain the amplitudes for $\bar{B} \rightarrow V_{1L}V_{2L}$ decays from the Hamiltonian, the matrix elements of the operators Q_i have to be computed in QCD factorization [6,7,8]. To lowest order the matrix elements are expressed in terms of $\bar{B} \rightarrow V$ form factors and vector-meson decay constants. The required form factors are defined by (see e.g. [22])

$$\begin{aligned} \langle V(p, \epsilon) | \bar{q} \gamma^\mu \gamma_5 b | \bar{B}(p_B) \rangle &= 2m_V A_0(q^2) \frac{\epsilon \cdot q}{q^2} q^\mu + (m_B + m_V) A_1(q^2) \left[\epsilon^\mu - \frac{\epsilon \cdot q}{q^2} q^\mu \right] \\ &\quad - A_2(q^2) \frac{\epsilon \cdot q}{m_B + m_V} \left[(p_B + p)^\mu - \frac{m_B^2 - m_V^2}{q^2} q^\mu \right] \end{aligned} \quad (3)$$

$$\langle V(p, \epsilon) | \bar{q} \gamma^\mu b | \bar{B}(p_B) \rangle = -2i \frac{V(q^2)}{m_B + m_V} \varepsilon^{\mu\nu\rho\sigma} p_{B\nu} p_\rho \epsilon_\sigma \quad (4)$$

where the momentum transfer is $q = p_B - p$ and the totally antisymmetric tensor $\varepsilon^{\mu\nu\rho\sigma}$ is normalized by $\varepsilon^{0123} = -1$.

The vector-meson decay constant f_V is given by

$$\langle V(q, \eta) | \bar{q} \gamma_\mu q' | 0 \rangle = -i f_V m_V \eta_\mu \quad (5)$$

for a vector meson with flavour content $V = \bar{q}' q$. The corresponding matrix element where $\gamma_\mu \rightarrow \gamma_\mu \gamma_5$ is zero. For energetic vector mesons $V(p, \epsilon)$ with longitudinal polarization

$$\epsilon^\mu = \frac{p^\mu}{m_V} \quad (6)$$

up to corrections of second order in m_V/m_B .

The factorized matrix element of a $(V - A) \otimes (V - A)$ operator then reads to lowest order (α_s^0)

$$\langle V_{1L} V_{2L} | (\bar{q}_1 b)_{V-A} (\bar{q}_2 q'_2)_{V-A} | \bar{B}_q \rangle = i m_B^2 A_0^{B \rightarrow V_1}(m_{V_2}^2) f_{V_2} \quad (7)$$

where $V_1 = \bar{q} q_1$ and $V_2 = \bar{q}'_2 q_2$ ($q_1 \neq q_2$).

The corrections at higher order in α_s are expressed in terms of calculable hard-scattering kernels and meson light-cone distribution amplitudes. The latter quantities enter through the meson projectors in momentum space. For the B meson this projector is given by

$$b\bar{q} = \frac{i f_B}{4} (\not{p}_B + m_B) \gamma_5 [\phi_{B1}(\xi) + \phi_{B2}(\xi) \not{n}] \quad (8)$$

In our notation $(b\bar{q})$ denotes a matrix in Dirac space displaying the flavour composition of a \bar{B}_q meson in the initial state. The 4-vector $n^\mu = (1, 0, 0, -1)$ is chosen to be in the direction of the recoiling meson V_1 . The parameter ξ is the light-cone momentum fraction of the spectator quark \bar{q} . The distribution amplitudes are normalized as

$$\int_0^1 d\xi \phi_{B1}(\xi) = 1, \quad \int_0^1 d\xi \phi_{B2}(\xi) = 0 \quad (9)$$

In the present analysis ϕ_{B2} does not enter the results and ϕ_{B1} appears only through the first inverse moment

$$\int_0^1 d\xi \frac{\phi_{B1}}{\xi} = \frac{m_B}{\lambda_B} \quad (10)$$

which defines the hadronic parameter $\lambda_B = \mathcal{O}(\Lambda_{QCD})$. Colour indices have been suppressed in writing (8). They are taken into account by replacing $b\bar{q} \rightarrow b_i\bar{q}_j$ and including a factor of δ_{ij}/N_c on the right-hand side.

For a longitudinally polarized vector meson in the final state with flavour content \bar{q}_2q_1 and momentum p , the projector can be written as [23]

$$q_2\bar{q}_1 = \frac{if_V}{4} \not{p} \phi_{\parallel}(x) - \frac{if_V^{\perp}}{4} m_V \frac{k_2 \cdot k_1}{k_2 \cdot k_1} \Phi_v(x) \quad (11)$$

Here x is the momentum fraction of the final-state quark q_1 and

$$k_1^{\mu} = xp^{\mu} + k_{\perp}^{\mu} + \frac{\vec{k}_{\perp}^2}{2xm_B} n^{\mu} \quad (12)$$

$$k_2^{\mu} = \bar{x}p^{\mu} - k_{\perp}^{\mu} + \frac{\vec{k}_{\perp}^2}{2\bar{x}m_B} n^{\mu} \quad (13)$$

(with $\bar{x} = 1 - x$) are the momenta of q_1 and \bar{q}_2 , respectively. n^{μ} is a light-like vector with spatial direction opposite to p^{μ} : If $p \sim n_+$ ($p \sim n_-$) then $n = n_-$ ($n = n_+$), where $n_{\pm}^{\mu} = (1, 0, 0, \pm 1)$.

The function $\phi_{\parallel}(x)$ is the light-cone distribution amplitude of leading twist for a longitudinal vector meson. The subleading-twist amplitude $\Phi_v(x)$ has been treated in (11) in the Wandzura-Wilczek approximation. It gives rise to contributions suppressed by one power of Λ_{QCD}/m_B . We will nevertheless include it in order to estimate the impact of this particular source of power corrections to factorization in the heavy-quark limit.

The functions ϕ_{\parallel} and Φ_v can be expanded in terms of Gegenbauer and Legendre polynomials, respectively,

$$\phi_{\parallel}(x) = 6x\bar{x} \sum_{n=0}^{\infty} \alpha_n C_n^{3/2}(2x-1) \quad (14)$$

$$\Phi_v(x) = 3 \sum_{n=0}^{\infty} \alpha_{n\perp} P_{n+1}(2x-1) \quad (15)$$

where $\alpha_0 = \alpha_{0\perp} = 1$. In the Wandzura-Wilczek approximation Φ_v can be expressed in terms of the twist-2 wave function of a transversely polarized vector meson, ϕ_{\perp} , as

$$\Phi_v(x) = \int_0^x du \frac{\phi_{\perp}(u)}{\bar{u}} - \int_x^1 du \frac{\phi_{\perp}(u)}{u} \quad (16)$$

ϕ_{\perp} has an expansion similar to (14) and this leads to (15).

Note that (16) implies

$$\int_0^1 dx \Phi_v(x) = 0 \quad (17)$$

even though $\Phi_v(x)$ is not necessarily antisymmetric under $x \leftrightarrow \bar{x}$ for general $\alpha_{n\perp}$. The normalization of $\phi_{\parallel,\perp}$ is $\int_0^1 dx \phi_{\parallel,\perp}(x) = 1$.

For phenomenological applications we shall truncate the expansions of ϕ_{\parallel} and Φ_v and use, for a particular meson V ,

$$\phi_{\parallel}^V(x) = 6x\bar{x} [1 + \alpha_1^V 3(2x-1) + \alpha_2^V 6(5x^2 - 5x + 1)] \quad (18)$$

$$\Phi_v^V(x) = 3(2x-1) \quad (19)$$

Taking the vacuum-to-meson matrix element of a local current, the projector (11) reproduces (5), (6)

$$\langle V(p) | \bar{q}_1 \gamma_\mu q_2 | 0 \rangle = - \int_0^1 dx \text{tr} \gamma_\mu q_2 \bar{q}_1 = -if_V p_\mu \quad (20)$$

and

$$\langle V(p) | \bar{q}_1 \Gamma q_2 | 0 \rangle = 0 \quad (21)$$

for $\Gamma = 1, \gamma_5, \gamma_\mu \gamma_5$.

3 QCD factorization in $B \rightarrow V_L V_L$ decays

The amplitudes for the $\Delta S = 0$ decay of a \bar{B} meson into a pair of light vector mesons with longitudinal polarization can be conveniently expressed as follows (the case of $\Delta S = 1$ is obtained by replacing $d \leftrightarrow s$):

$$\langle V_{1L} V_{2L} | \mathcal{H}_{\text{eff}}^{\Delta S=0} | \bar{B} \rangle = \frac{G_F}{\sqrt{2}} \sum_{p=u,c} \lambda_p \langle V_{1L} V_{2L} | \mathcal{T}_p^d + \mathcal{T}_p^{\text{ann},d} | \bar{B} \rangle \quad (22)$$

where

$$\begin{aligned} \mathcal{T}_p^d &= a_1(V_1 V_2) \delta_{pu} (\bar{u}b)_{V-A} \otimes (\bar{d}u)_{V-A} \\ &+ a_2(V_1 V_2) \delta_{pu} (\bar{d}b)_{V-A} \otimes (\bar{u}u)_{V-A} \\ &+ a_3(V_1 V_2) \sum_q (\bar{d}b)_{V-A} \otimes (\bar{q}q)_{V-A} \\ &+ a_4^p(V_1 V_2) \sum_q (\bar{q}b)_{V-A} \otimes (\bar{d}q)_{V-A} \\ &+ a_5(V_1 V_2) \sum_q (\bar{d}b)_{V-A} \otimes (\bar{q}q)_{V+A} \\ &+ a_7(V_1 V_2) \sum_q (\bar{d}b)_{V-A} \otimes \frac{3}{2} e_q (\bar{q}q)_{V+A} \\ &+ a_9(V_1 V_2) \sum_q (\bar{d}b)_{V-A} \otimes \frac{3}{2} e_q (\bar{q}q)_{V-A} \\ &+ a_{10}^p(V_1 V_2) \sum_q (\bar{q}b)_{V-A} \otimes \frac{3}{2} e_q (\bar{d}q)_{V-A} \end{aligned} \quad (23)$$

Here the summation is over $q = u, d, s$. The symbol \otimes indicates that the matrix elements of the operators in \mathcal{T}_p^d are to be evaluated in factorized form [6]. The factorization coefficients a_i include hard QCD corrections to the B -decay matrix elements at NLO, as well as electroweak effects in the systematic approximation of [6]. Note that structures with scalar and pseudoscalar currents are absent in (23), in contrast to the case of $B \rightarrow K\pi$ considered in [6]. Because (pseudo)scalar currents cannot create a vector meson from the vacuum, these structures can give no contribution to $B \rightarrow VV$ decays.

The term $\mathcal{T}_p^{\text{ann},d}$ in (22) describes the effects of weak annihilation. These are power suppressed in the heavy-quark limit and cannot be computed in QCD factorization. We shall use model calculations to estimate this important class of power corrections to the leading, factorizable amplitudes. Weak annihilation will be discussed in Section 3.3.

3.1 Results for the parameters a_i

The factorization coefficients can be written as $a_i = a_{i,\text{I}} + a_{i,\text{II}}$. We find

$$\begin{aligned}
a_{1,\text{I}} &= C_1 + \frac{C_2}{N_c} \left[1 + \frac{C_F \alpha_s}{4\pi} V_V \right], & a_{1,\text{II}} &= \frac{C_2}{N_c} \frac{C_F \pi \alpha_s}{N_c} H_{V_1 V_2}, \\
a_{2,\text{I}} &= C_2 + \frac{C_1}{N_c} \left[1 + \frac{C_F \alpha_s}{4\pi} V_V \right], & a_{2,\text{II}} &= \frac{C_1}{N_c} \frac{C_F \pi \alpha_s}{N_c} H_{V_1 V_2}, \\
a_{3,\text{I}} &= C_3 + \frac{C_4}{N_c} \left[1 + \frac{C_F \alpha_s}{4\pi} V_V \right], & a_{3,\text{II}} &= \frac{C_4}{N_c} \frac{C_F \pi \alpha_s}{N_c} H_{V_1 V_2}, \\
a_{4,\text{I}}^p &= C_4 + \frac{C_3}{N_c} \left[1 + \frac{C_F \alpha_s}{4\pi} V_V \right] - \frac{C_5}{N_c} \frac{C_F \alpha_s}{4\pi} r_{\perp}^V V_V^{\perp} \\
&\quad + \frac{C_F \alpha_s}{4\pi N_c} (P_{V,2}^p - r_{\perp}^V P_{V,3}^p), & a_{4,\text{II}} &= \frac{C_3}{N_c} \frac{C_F \pi \alpha_s}{N_c} H_{V_1 V_2}, \\
a_{5,\text{I}} &= C_5 + \frac{C_6}{N_c} \left[1 + \frac{C_F \alpha_s}{4\pi} (-V_V') \right], & a_{5,\text{II}} &= \frac{C_6}{N_c} \frac{C_F \pi \alpha_s}{N_c} (-H'_{V_1 V_2}), \\
a_{7,\text{I}}^p &= C_7 + \frac{C_8}{N_c} \left[1 + \frac{C_F \alpha_s}{4\pi} (-V_V') \right] + \frac{\alpha}{9\pi} P_{V,n}^{p,\text{EW}}, & a_{7,\text{II}} &= \frac{C_8}{N_c} \frac{C_F \pi \alpha_s}{N_c} (-H'_{V_1 V_2}), \\
a_{9,\text{I}}^p &= C_9 + \frac{C_{10}}{N_c} \left[1 + \frac{C_F \alpha_s}{4\pi} V_V \right] + \frac{\alpha}{9\pi} P_{V,n}^{p,\text{EW}}, & a_{9,\text{II}} &= \frac{C_{10}}{N_c} \frac{C_F \pi \alpha_s}{N_c} H_{V_1 V_2}, \\
a_{10,\text{I}}^p &= C_{10} + \frac{C_9}{N_c} \left[1 + \frac{C_F \alpha_s}{4\pi} V_V \right] - \frac{C_7}{N_c} \frac{C_F \alpha_s}{4\pi} r_{\perp}^V V_V^{\perp} \\
&\quad + \frac{\alpha}{9\pi N_c} (P_{V,2}^{p,\text{EW}} - r_{\perp}^V P_{V,3}^{p,\text{EW}}), & a_{10,\text{II}} &= \frac{C_9}{N_c} \frac{C_F \pi \alpha_s}{N_c} H_{V_1 V_2} \quad (24)
\end{aligned}$$

where $C_i \equiv C_i(\mu)$, $\alpha_s \equiv \alpha_s(\mu)$, $C_F = (N_c^2 - 1)/(2N_c)$, and $N_c = 3$. The hadronic quantities $V_V^{(\prime)}$, $H_{V_1 V_2}^{(\prime)}$, $P_{V,2}^p$, $P_{V,3}^p$, $P_{V,2}^{p,\text{EW}}$, $P_{V,3}^{p,\text{EW}}$, and $P_{V,n}^{p,\text{EW}}$ are given below. All indices

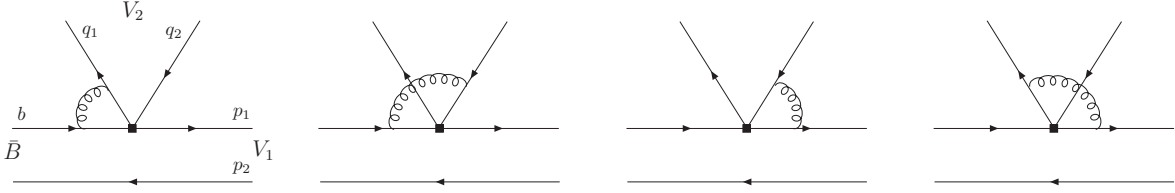


Figure 1: Vertex diagrams.

v in V_V , P_V , r^V are understood to refer to the emitted meson V_2 .

Contributions suppressed by one power of Λ_{QCD}/m_b that arise from the twist-3 component of the vector-meson wave function have been included in the above expressions. They are related to the scalar penguin operator $(\bar{q}b)_{S-P}(\bar{s}q)_{S+P}$ and come with a factor

$$r_{\perp}^V(\mu) = \frac{2m_V f_V^{\perp}(\mu)}{m_b(\mu) f_V} = \frac{2m_V f_V^{\perp}(1\text{GeV})}{m_b(m_b) f_V} \left[\frac{\alpha_s(\mu)}{\alpha_s(m_b)} \right]^{-3C_F/\beta_0} \left[\frac{\alpha_s(\mu)}{\alpha_s(1\text{GeV})} \right]^{C_F/\beta_0} \quad (25)$$

Here $m_b(\mu)$ is the \overline{MS} -mass of the b quark at scale μ , and $\beta_0 = 23/3$ for $f = 5$ flavours of quarks.

3.1.1 Vertex and penguin contributions

The vertex corrections (Fig. 1) are given by

$$\begin{aligned} V_V &= 12 \ln \frac{m_b}{\mu} - 18 + \int_0^1 dx g(x) \phi_{\parallel}^V(x), \\ V_V' &= 12 \ln \frac{m_b}{\mu} - 6 + \int_0^1 dx g(1-x) \phi_{\parallel}^V(x), \\ g(x) &= 3 \left(\frac{1-2x}{1-x} \ln x - i\pi \right) \\ &\quad + \left[2 L_2(x) - \ln^2 x + \frac{2 \ln x}{1-x} - (3 + 2i\pi) \ln x - (x \leftrightarrow 1-x) \right] \end{aligned} \quad (26)$$

$$V_V^{\perp} = \int_0^1 dx \left[2 L_2(x) - \ln^2 x - (1 + 2i\pi) \ln x - (x \leftrightarrow 1-x) \right] \Phi_v^V(x) \quad (27)$$

where $L_2(x)$ is the dilogarithm

$$L_2(x) = - \int_0^x dt \frac{\ln(1-t)}{t} \quad (28)$$

The expansion of ϕ_{\parallel}^V in Gegenbauer polynomials gives

$$\int_0^1 dx g(x) \phi_{\parallel}^V(x) = -\frac{1}{2} - 3i\pi + \left(\frac{11}{2} - 3i\pi \right) \alpha_1^V - \frac{21}{20} \alpha_2^V + \dots \quad (29)$$

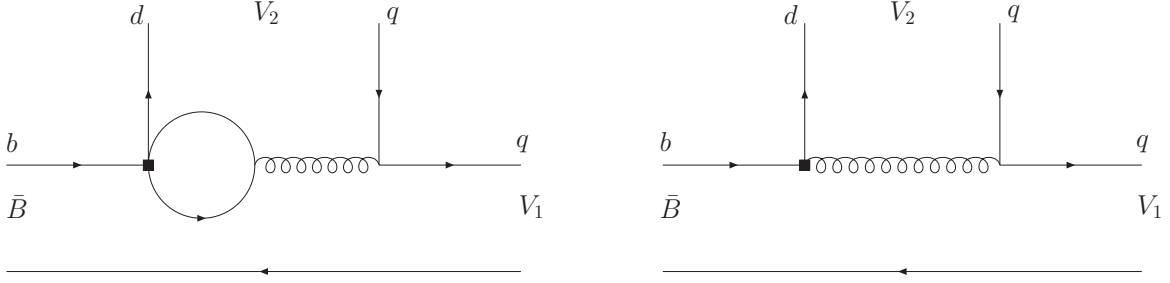


Figure 2: Penguin diagrams.

Replacing $g(x)$ by $g(1-x)$ leads to a change of sign in front of the odd Gegenbauer coefficients on the right-hand side.

Next, the penguin contributions (Fig. 2) are

$$\begin{aligned}
P_{V,2}^p &= C_1 \left[\frac{4}{3} \ln \frac{m_b}{\mu} + \frac{2}{3} - G_V(s_p) \right] + C_3 \left[\frac{8}{3} \ln \frac{m_b}{\mu} + \frac{4}{3} - G_V(0) - G_V(1) \right] \\
&\quad + (C_4 + C_6) \left[\frac{20}{3} \ln \frac{m_b}{\mu} - 3G_V(0) - G_V(s_c) - G_V(1) \right] \\
&\quad - 2C_{8g}^{\text{eff}} \int_0^1 \frac{dx}{1-x} \phi_{\parallel}^V(x), \\
P_{V,2}^{p,\text{EW}} &= (C_1 + N_c C_2) \left[\frac{4}{3} \ln \frac{m_b}{\mu} + \frac{2}{3} - G_V(s_p) \right] - 3C_{7\gamma}^{\text{eff}} \int_0^1 \frac{dx}{1-x} \phi_{\parallel}^V(x) \quad (30)
\end{aligned}$$

where $s_u = 0$ and $s_c = (m_c/m_b)^2$. Small contributions from the electroweak coefficients C_7, \dots, C_{10} are consistently neglected in $P_{V,2}^p$ within our approximation scheme. Also, the very small corrections from C_3, \dots, C_6 in $P_{V,2}^{p,\text{EW}}$ (and in $P_{V,3}^{p,\text{EW}}$, see (35) below) are omitted for simplicity.

The function $G_V(s)$ is

$$G_V(s) = \int_0^1 dx G(s - i\epsilon, 1-x) \phi_{\parallel}^V(x), \quad (31)$$

$$\begin{aligned}
G(s, x) &= -4 \int_0^1 du u(1-u) \ln[s - u(1-u)x] \\
&= \frac{2(12s + 5x - 3x \ln s)}{9x} - \frac{4\sqrt{4s-x}(2s+x)}{3x^{3/2}} \arctan \sqrt{\frac{x}{4s-x}} \quad (32)
\end{aligned}$$

Expanding in Gegenbauer moments one finds

$$\begin{aligned}
G_V(s_c) &= \frac{5}{3} - \frac{2}{3} \ln s_c + \frac{\alpha_1^V}{2} + \frac{\alpha_2^V}{5} + \frac{4}{3} (8 + 9\alpha_1^V + 9\alpha_2^V) s_c \\
&\quad + 2(8 + 63\alpha_1^V + 214\alpha_2^V) s_c^2 - 24(9\alpha_1^V + 80\alpha_2^V) s_c^3 + 2880\alpha_2^V s_c^4 \\
&\quad - \frac{2}{3} \sqrt{1 - 4s_c} \left[1 + 2s_c + 6(4 + 27\alpha_1^V + 78\alpha_2^V) s_c^2 \right. \\
&\quad \left. - 36(9\alpha_1^V + 70\alpha_2^V) s_c^3 + 4320\alpha_2^V s_c^4 \right] (2 \operatorname{arctanh} \sqrt{1 - 4s_c} - i\pi) \\
&\quad + 12s_c^2 \left[1 + 3\alpha_1^V + 6\alpha_2^V - \frac{4}{3} (1 + 9\alpha_1^V + 36\alpha_2^V) s_c \right. \\
&\quad \left. + 18(\alpha_1^V + 10\alpha_2^V) s_c^2 - 240\alpha_2^V s_c^3 \right] (2 \operatorname{arctanh} \sqrt{1 - 4s_c} - i\pi)^2 + \dots, \\
G_V(0) &= \frac{5}{3} + \frac{2i\pi}{3} + \frac{\alpha_1^V}{2} + \frac{\alpha_2^V}{5} + \dots, \\
G_V(1) &= \frac{85}{3} - 6\sqrt{3}\pi + \frac{4\pi^2}{9} - \left(\frac{155}{2} - 36\sqrt{3}\pi + 12\pi^2 \right) \alpha_1^V \\
&\quad + \left(\frac{7001}{5} - 504\sqrt{3}\pi + 136\pi^2 \right) \alpha_2^V + \dots
\end{aligned} \tag{33}$$

The function $G_V(s)$ and its expansion in Gegenbauer moments have the same form as $G_K(s)$ in the case of $B \rightarrow K\pi$ discussed in [6]. Likewise the integrals proportional to $C_{7\gamma}^{\text{eff}}$ and C_{8g}^{eff} in (30) are similar to those in $B \rightarrow K\pi$. They read

$$\int_0^1 \frac{dx}{1-x} \phi_{\parallel}^V(x) = 3(1 + \alpha_1^V + \alpha_2^V + \dots) \tag{34}$$

The twist-3 terms from the penguin diagrams are obtained from the twist-2 terms by the replacement $\phi_{\parallel}^V(x) \rightarrow \Phi_v^V(x)$, except for the terms proportional to $C_{7\gamma}^{\text{eff}}$ and C_{8g}^{eff} . Here the factor of $(1-x)$ in the denominator of the integral in (30) is canceled by the twist-3 projection. An important difference between the twist-3 penguin contributions in $B \rightarrow V_L V_L$ and $B \rightarrow K\pi$ arises from the different properties of the twist-3 wave functions in these two cases. Since $\int_0^1 dx \Phi_v^V(x) = 0$ it follows that the contributions from $C_{7\gamma}^{\text{eff}}$ and C_{8g}^{eff} vanish in the former case. The same holds for all x -independent constants in the hard-scattering kernel, in particular for the scale and scheme dependent terms. We then find

$$\begin{aligned}
P_{V,3}^p &= - \left[C_1 \hat{G}_V(s_p) + C_3 (\hat{G}_V(0) + \hat{G}_V(1)) + (C_4 + C_6) (3\hat{G}_V(0) + \hat{G}_V(s_c) + \hat{G}_V(1)) \right] \\
P_{V,3}^{p,\text{EW}} &= -(C_1 + N_c C_2) \hat{G}_V(s_p)
\end{aligned} \tag{35}$$

with

$$\hat{G}_V(s) = \int_0^1 dx G(s - i\epsilon, 1 - x) \Phi_v^V(x) \quad (36)$$

Using the asymptotic form of the wave function $\Phi_v^V(x) = 3(2x - 1)$ leads to

$$\begin{aligned} \hat{G}_V(s_c) &= 1 - 36s_c + 12s_c\sqrt{1 - 4s_c} (2 \operatorname{arctanh}\sqrt{1 - 4s_c} - i\pi) \\ &\quad - 12s_c^2 (2 \operatorname{arctanh}\sqrt{1 - 4s_c} - i\pi)^2, \\ \hat{G}_V(0) &= 1, \quad \hat{G}_V(1) = \frac{4}{3}\pi^2 + 4\sqrt{3}\pi - 35 \end{aligned} \quad (37)$$

Finally, we give the electromagnetic penguin contributions $P_{V,n}^{p,\text{EW}}$ ($p = u, c$). For intermediate charm, $p = c$, these are calculable in perturbation theory and read

$$P_{V,n}^{c,\text{EW}} = (C_1 + N_c C_2) \left[\frac{4}{3} \ln \frac{m_b}{\mu} + \frac{2}{3} + \frac{4}{3} \ln \frac{m_c}{m_b} \right] - 3C_{7\gamma}^{\text{eff}} \quad (38)$$

In the case of the up-quark loop, $p = u$, the amplitude becomes sensitive to additional long-distance dynamics, which is not strictly calculable. Using a suitable hadronic representation of the light-quark loop, we estimate

$$\begin{aligned} P_{V,n}^{u,\text{EW}} &= (C_1 + N_c C_2) \left[\frac{4}{3} \ln \frac{m_b}{\mu} - \frac{10}{9} + \frac{4\pi^2}{3} \sum_{r=\rho,\omega} \frac{f_r^2}{m_V^2 - m_r^2 + im_r\Gamma_r} \right. \\ &\quad \left. - \frac{2\pi}{3} \frac{m_V^2}{t_c} i + \frac{2}{3} \ln \frac{m_V^2}{m_b^2} + \frac{2}{3} \frac{t_c - m_V^2}{t_c} \ln \frac{t_c - m_V^2}{m_V^2} \right] - 3C_{7\gamma}^{\text{eff}} \end{aligned} \quad (39)$$

where $t_c = 4\pi^2(f_\rho^2 + f_\omega^2)$. This point is discussed further in appendix A.

The authors of [23] factorize the term (39) into a short-distance and a long-distance part, separated by a scale ν . The short-distance part is equivalent to (38) with m_c replaced by ν . The long-distance part is not considered explicitly in [23]. Our treatment is consistent with the framework of [23], but supplies a concrete model representation for the long-distance contribution of the electromagnetic penguin.

3.1.2 Hard spectator scattering

The hard spectator interactions (Fig. 3) determining the coefficients $a_{i,II}$ in (24) are governed by the quantities

$$H_{V_1 V_2} = \frac{f_B f_{V_1}}{m_B^2 A_0^{B \rightarrow V_1}(0)} \int_0^1 \frac{d\xi}{\xi} \Phi_B(\xi) \int_0^1 \frac{dx}{\bar{x}} \phi_{\parallel}^{V_2}(x) \int_0^1 \frac{dy}{\bar{y}} \left[\phi_{\parallel}^{V_1}(y) + r_{\perp}^{V_1} \frac{\bar{x}}{x} \Phi_v^{V_1}(y) \right] \quad (40)$$

$$H'_{V_1 V_2} = \frac{f_B f_{V_1}}{m_B^2 A_0^{B \rightarrow V_1}(0)} \int_0^1 \frac{d\xi}{\xi} \Phi_B(\xi) \int_0^1 \frac{dx}{x} \phi_{\parallel}^{V_2}(x) \int_0^1 \frac{dy}{\bar{y}} \left[\phi_{\parallel}^{V_1}(y) + r_{\perp}^{V_1} \frac{x}{\bar{x}} \Phi_v^{V_1}(y) \right] \quad (41)$$

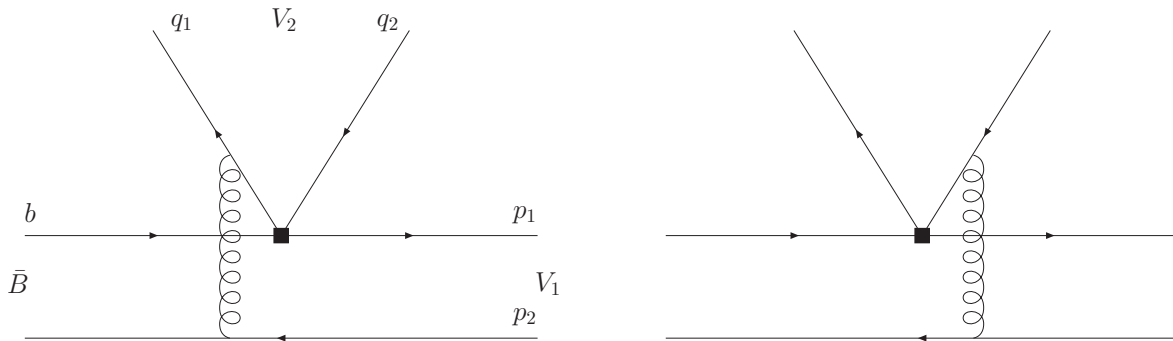


Figure 3: Hard spectator diagrams.

Strictly speaking, only the twist-2 components $\phi_{||}$ of the vector meson distribution amplitudes contribute at leading power and are consistently calculable in the present approach. The twist-3 part described by Φ_v leads to terms with logarithmic endpoint singularities, but these terms are suppressed by one power of Λ/m_b . We shall include them in our analysis using a simple model, in order to estimate the potential impact of power corrections from this source. Following [6], we parametrize the endpoint singularity by

$$X_H = \int_0^1 \frac{dy}{\bar{y}} = (1 + \rho_H e^{i\phi_H}) \ln \frac{m_B}{\Lambda_h} \quad (42)$$

The logarithm comes from cutting off the lower range of integration at $\bar{y}_{min} = \Lambda_h/m_B$, and ρ_H , ϕ_H are real model parameters to allow for a complex X_H and a deviation from the default value $\ln(m_B/\Lambda_h)$. The integral over Φ_v in (40), (41) then becomes

$$\int_0^1 \frac{dy}{\bar{y}} \Phi_v(y) = 3(X_H - 2) \quad (43)$$

Throughout we use $\mu_h = \sqrt{\Lambda_h \mu}$ with $\Lambda_h = 0.5 \text{ GeV}$ as the scale in the spectator-scattering contributions.

3.2 $\bar{B} \rightarrow V_{1L} V_{2L}$ decay amplitudes

The transition operators \mathcal{T}^d , \mathcal{T}^s describe a total of 28 two-body decays of B^- , \bar{B}_d and \bar{B}_s into the charmless vector mesons K^{*+} , K^{*-} , K^{*0} , \bar{K}^{*0} , ρ^+ , ρ^- , ρ^0 , ω and ϕ . There are 15 $\Delta S = 0$ ($b \rightarrow d$) and 13 $\Delta S = 1$ ($b \rightarrow s$) transitions. In this section we give the expressions for the amplitudes of these processes in terms of the factorization coefficients a_i . All light vector mesons are taken to be longitudinally polarized, that is, $\rho^- \rho^0$ here means $\rho_L^- \rho_L^0$. We use the abbreviation

$$A_{V_1 V_2} = i \frac{G_F}{\sqrt{2}} m_B^2 A_0^{B \rightarrow V_1}(m_{V_2}^2) f_{V_2} \quad (44)$$

suppressing the dependence of $A_{V_1 V_2}$ on the B -meson flavour in the notation.

The decay amplitudes, up to the factor (44), are conveniently obtained from the transition operator by the following 'bosonization' of the bilinear quark currents in (23):

$$\begin{aligned}(\bar{u}b)_{V-A} &= \frac{B^- \rho^0 + B^- \omega}{\sqrt{2}} + \bar{B}_d \rho^+ + \bar{B}_s K^{*+} \\(\bar{d}b)_{V-A} &= B^- \rho^- + \frac{\bar{B}_d \omega - \bar{B}_d \rho^0}{\sqrt{2}} + \bar{B}_s K^{*0} \\(\bar{s}b)_{V-A} &= B^- K^{*-} + \bar{B}_d \bar{K}^{*0} + \bar{B}_s \phi\end{aligned}\tag{45}$$

$$(\bar{d}u)_V = \rho^-, \quad (\bar{u}d)_V = \rho^+, \quad (\bar{s}d)_V = \bar{K}^{*0}\tag{46}$$

$$(\bar{d}s)_V = K^{*0}, \quad (\bar{s}u)_V = K^{*-}, \quad (\bar{u}s)_V = K^{*+}\tag{47}$$

$$(\bar{u}u)_V = \frac{\rho^0 + \omega}{\sqrt{2}}, \quad (\bar{d}d)_V = \frac{\omega - \rho^0}{\sqrt{2}}, \quad (\bar{s}s)_V = \phi\tag{48}$$

In our notation the charge of B mesons (light mesons) corresponds to that of particles in the initial (final) state. Note that the axial vector parts of the light-quark currents don't contribute for final-state vector mesons. Insertion of these expressions in \mathcal{T}^d (\mathcal{T}^s) from eq. (23) generates all $\Delta S = 0$ ($\Delta S = 1$) amplitudes. For a specific process $\bar{B} \rightarrow V_1 V_2$ the amplitude is found as the coefficient of $(\bar{B} V_1) V_2$ (and of $(\bar{B} V_2) V_1$ if $V_1 \neq V_2$). This procedure automatically keeps track of all sign and Clebsch-Gordan factors. Note, however, that an extra symmetry factor of 2 has to be included for amplitudes with two identical particles in the final state. From the structure of $\mathcal{T}^{d(s)}$ it follows that the coefficients a_3 , a_5 and a_7^p , a_9^p always appear in the combination $a_3 + a_5$ and $a_7^p + a_9^p$, respectively. Representative numerical values for the coefficients a_i can be found in appendix B.

The $\Delta S = 0$ transition amplitudes then read (a summation over $p = u, c$ is understood):

$$\sqrt{2} \mathcal{A}(B^- \rightarrow \rho^- \rho^0) = \left[\lambda_u (a_1 + a_2) + \frac{3}{2} \lambda_p (a_7^p + a_9^p + a_{10}^p) \right] A_{\rho\rho}\tag{49}$$

$$\begin{aligned}\sqrt{2} \mathcal{A}(B^- \rightarrow \rho^- \omega) &= [\lambda_u a_1 + \lambda_p (a_4^p + a_{10}^p)] A_{\omega\rho} \\ &+ \left[\lambda_u a_2 + \lambda_p \left(a_4^p + 2(a_3 + a_5) + \frac{1}{2}(a_7^p + a_9^p - a_{10}^p) \right) \right] A_{\rho\omega}\end{aligned}\tag{50}$$

$$\mathcal{A}(B^- \rightarrow \rho^- \phi) = \lambda_p \left[a_3 + a_5 - \frac{1}{2}(a_7^p + a_9^p) \right] A_{\rho\phi}\tag{51}$$

$$\mathcal{A}(B^- \rightarrow K^{*-} K^{*0}) = \lambda_p \left[a_4^p - \frac{1}{2} a_{10}^p \right] A_{K^* K^*}\tag{52}$$

$$\mathcal{A}(\bar{B}_d \rightarrow \rho^0 \rho^0) = \left[-\lambda_u a_2 + \lambda_p \left(a_4^p - \frac{3}{2}(a_7^p + a_9^p) - \frac{1}{2} a_{10}^p \right) \right] A_{\rho\rho}\tag{53}$$

$$\begin{aligned} \mathcal{A}(\bar{B}_d \rightarrow \rho^0 \omega) &= \frac{1}{2} \left[\lambda_u a_2 + \lambda_p \left(-a_4^p + \frac{3}{2}(a_7^p + a_9^p) + \frac{1}{2}a_{10}^p \right) \right] A_{\omega\rho} \\ &\quad - \frac{1}{2} \left[\lambda_u a_2 + \lambda_p \left(a_4^p + 2(a_3 + a_5) + \frac{1}{2}(a_7^p + a_9^p - a_{10}^p) \right) \right] A_{\rho\omega} \end{aligned} \quad (54)$$

$$\mathcal{A}(\bar{B}_d \rightarrow \omega\omega) = \left[\lambda_u a_2 + \lambda_p \left(a_4^p + 2(a_3 + a_5) + \frac{1}{2}(a_7^p + a_9^p - a_{10}^p) \right) \right] A_{\omega\omega} \quad (55)$$

$$\sqrt{2}\mathcal{A}(\bar{B}_d \rightarrow \rho^0 \phi) = -\lambda_p \left[a_3 + a_5 - \frac{1}{2}(a_7^p + a_9^p) \right] A_{\rho\phi} \quad (56)$$

$$\sqrt{2}\mathcal{A}(\bar{B}_d \rightarrow \omega\phi) = \lambda_p \left[a_3 + a_5 - \frac{1}{2}(a_7^p + a_9^p) \right] A_{\omega\phi} \quad (57)$$

$$\mathcal{A}(\bar{B}_d \rightarrow \rho^+ \rho^-) = [\lambda_u a_1 + \lambda_p (a_4^p + a_{10}^p)] A_{\rho\rho} \quad (58)$$

$$\mathcal{A}(\bar{B}_d \rightarrow \bar{K}^{*0} K^{*0}) = \lambda_p \left[a_4^p - \frac{1}{2}a_{10}^p \right] A_{K^*K^*} \quad (59)$$

$$\sqrt{2}\mathcal{A}(\bar{B}_s \rightarrow K^{*0} \rho^0) = \left[\lambda_u a_2 + \lambda_p \left(-a_4^p + \frac{3}{2}(a_7^p + a_9^p) + \frac{1}{2}a_{10}^p \right) \right] A_{K^*\rho} \quad (60)$$

$$\sqrt{2}\mathcal{A}(\bar{B}_s \rightarrow K^{*0} \omega) = \left[\lambda_u a_2 + \lambda_p \left(a_4^p + 2(a_3 + a_5) + \frac{1}{2}(a_7^p + a_9^p - a_{10}^p) \right) \right] A_{K^*\omega} \quad (61)$$

$$\mathcal{A}(\bar{B}_s \rightarrow K^{*0} \phi) = \lambda_p \left[a_4^p - \frac{1}{2}a_{10}^p \right] A_{\phi K^*} + \lambda_p \left[a_3 + a_5 - \frac{1}{2}(a_7^p + a_9^p) \right] A_{K^*\phi} \quad (62)$$

$$\mathcal{A}(\bar{B}_s \rightarrow K^{*+} \rho^-) = [\lambda_u a_1 + \lambda_p (a_4^p + a_{10}^p)] A_{K^*\rho} \quad (63)$$

The amplitudes for $\Delta S = 1$ transitions are found to be:

$$\sqrt{2}\mathcal{A}(B^- \rightarrow K^{*-} \rho^0) = [\lambda'_u a_1 + \lambda'_p (a_4^p + a_{10}^p)] A_{\rho K^*} + \left[\lambda'_u a_2 + \frac{3}{2}\lambda'_p (a_7^p + a_9^p) \right] A_{K^*\rho} \quad (64)$$

$$\begin{aligned} \sqrt{2}\mathcal{A}(B^- \rightarrow K^{*-} \omega) &= [\lambda'_u a_1 + \lambda'_p (a_4^p + a_{10}^p)] A_{\omega K^*} \\ &\quad + \left[\lambda'_u a_2 + \lambda'_p \left(2(a_3 + a_5) + \frac{1}{2}(a_7^p + a_9^p) \right) \right] A_{K^*\omega} \end{aligned} \quad (65)$$

$$\mathcal{A}(B^- \rightarrow K^{*-} \phi) = \lambda'_p \left[a_4^p + a_3 + a_5 - \frac{1}{2}(a_7^p + a_9^p + a_{10}^p) \right] A_{K^*\phi} \quad (66)$$

$$\mathcal{A}(B^- \rightarrow \bar{K}^{*0} \rho^-) = \lambda'_p \left[a_4^p - \frac{1}{2}a_{10}^p \right] A_{\rho K^*} \quad (67)$$

$$\sqrt{2}\mathcal{A}(\bar{B}_d \rightarrow \bar{K}^{*0}\rho^0) = \left[\lambda'_u a_2 + \frac{3}{2}\lambda'_p(a_7^p + a_9^p) \right] A_{K^*\rho} - \lambda'_p \left[a_4^p - \frac{1}{2}a_{10}^p \right] A_{\rho K^*} \quad (68)$$

$$\begin{aligned} \sqrt{2}\mathcal{A}(\bar{B}_d \rightarrow \bar{K}^{*0}\omega) &= \left[\lambda'_u a_2 + \lambda'_p \left(2(a_3 + a_5) + \frac{1}{2}(a_7^p + a_9^p) \right) \right] A_{K^*\omega} \\ &+ \lambda'_p \left[a_4^p - \frac{1}{2}a_{10}^p \right] A_{\omega K^*} \end{aligned} \quad (69)$$

$$\mathcal{A}(\bar{B}_d \rightarrow \bar{K}^{*0}\phi) = \lambda'_p \left[a_4^p + a_3 + a_5 - \frac{1}{2}(a_7^p + a_9^p + a_{10}^p) \right] A_{K^*\phi} \quad (70)$$

$$\mathcal{A}(\bar{B}_d \rightarrow K^{*-}\rho^+) = [\lambda'_u a_1 + \lambda'_p(a_4^p + a_{10}^p)] A_{\rho K^*} \quad (71)$$

$$\sqrt{2}\mathcal{A}(\bar{B}_s \rightarrow \rho^0\phi) = \left[\lambda'_u a_2 + \frac{3}{2}\lambda'_p(a_7^p + a_9^p) \right] A_{\phi\rho} \quad (72)$$

$$\sqrt{2}\mathcal{A}(\bar{B}_s \rightarrow \omega\phi) = \left[\lambda'_u a_2 + \lambda'_p \left(2(a_3 + a_5) + \frac{1}{2}(a_7^p + a_9^p) \right) \right] A_{\phi\omega} \quad (73)$$

$$\mathcal{A}(\bar{B}_s \rightarrow \phi\phi) = 2\lambda'_p \left[a_4^p + a_3 + a_5 - \frac{1}{2}(a_7^p + a_9^p + a_{10}^p) \right] A_{\phi\phi} \quad (74)$$

$$\mathcal{A}(\bar{B}_s \rightarrow K^{*+}K^{*-}) = [\lambda'_u a_1 + \lambda'_p(a_4^p + a_{10}^p)] A_{K^*K^*} \quad (75)$$

$$\mathcal{A}(\bar{B}_s \rightarrow \bar{K}^{*0}K^{*0}) = \lambda'_p \left[a_4^p - \frac{1}{2}a_{10}^p \right] A_{K^*K^*} \quad (76)$$

3.3 Weak annihilation amplitudes

The decay mechanism of weak annihilation (Fig. 4) gives contributions to the amplitudes for $B \rightarrow V_L V_L$ decays that are suppressed by Λ_{QCD}/m_b . These power corrections are not calculable in the usual factorization framework. This is indicated by end-point singularities from the integrals over light-cone momentum fractions in a hard-scattering ansatz. We shall use the model of [6], which is based on this ansatz together with a cut-off procedure, to estimate the impact of annihilation effects on the leading decay amplitudes. Following the notation of [6] we write

$$\langle V_{1L} V_{2L} | \mathcal{H}_{\text{eff}}^{\Delta S=0} | \bar{B} \rangle_{\text{ann}} = \frac{G_F}{\sqrt{2}} \sum_{p=u,c} \lambda_p \langle V_{1L} V_{2L} | \mathcal{T}_p^{\text{ann},d} | \bar{B} \rangle \quad (77)$$

with $\lambda_p = V_{pb} V_{pd}^*$ and

$$\begin{aligned} \mathcal{T}_p^{\text{ann},d} &= \delta_{up} (\delta_{rd} b_1 \sigma_u^u + \delta_{ru} b_2 \sigma_d^u) + b_3 \sigma_d^r + \delta_{rd} b_4 \text{tr}(\sigma) \\ &+ \frac{3}{2} b_3^{\text{EW}} e_r \sigma_d^r + \frac{3}{2} \delta_{rd} b_4^{\text{EW}} \text{tr}(Q\sigma) \end{aligned} \quad (78)$$

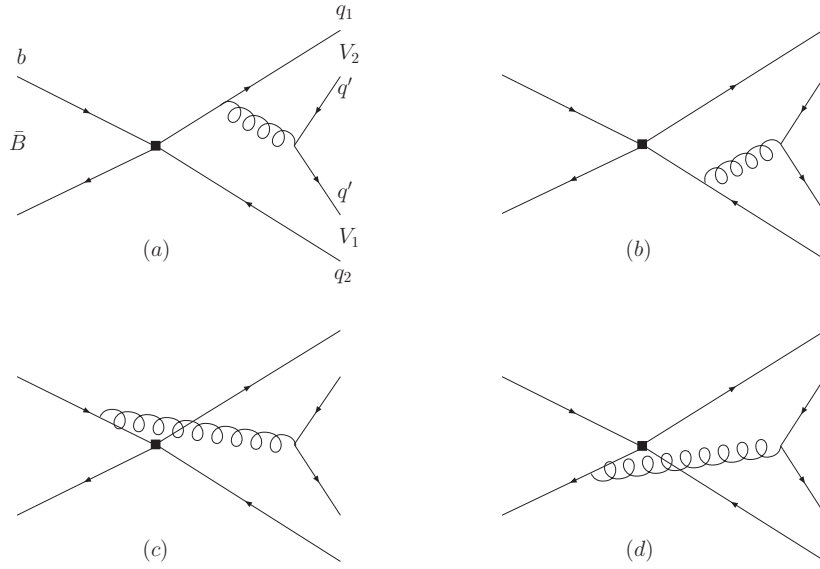


Figure 4: Annihilation diagrams.

Here the index $r = u, d, s$ denotes the flavour of the spectator quark in the B meson and $Q = \text{diag}(2/3, -1/3, -1/3)$. The corresponding formulas for $\Delta S = 1$ transitions are obtained by interchanging the labels $d \leftrightarrow s$ in the expressions (77), (78) for $\Delta S = 0$. In particular, λ_p is then replaced by $\lambda'_p = V_{pb}V_{ps}^*$.

The operators

$$\sigma_{q_1}^{q_2} = \sum_{q'=u,d,s} (\bar{q}' q_2) \times (\bar{q}_1 q') \quad (79)$$

encode the valence quarks of the final state mesons. Matrix elements of the product of currents in (79) are defined as

$$\langle V_{1L} V_{2L} | j_1 \times j_2 | \bar{B} \rangle \equiv ic f_B f_{V_1} f_{V_2} \quad (80)$$

where $c = 0, 1, \pm 1/\sqrt{2}$, etc., is the appropriate Clebsch-Gordan coefficient and symmetry factor, relating the currents j_1 and j_2 to the mesons V_1, V_2 . The coefficients b_i are given by

$$\begin{aligned} b_1 &= \frac{C_F}{N_c^2} C_1 A_1^i, & b_3 &= \frac{C_F}{N_c^2} \left[C_3 A_1^i + C_5 (A_3^i + A_3^f) + N_c C_6 A_3^f \right], \\ b_2 &= \frac{C_F}{N_c^2} C_2 A_1^i, & b_4 &= \frac{C_F}{N_c^2} \left[C_4 A_1^i + C_6 A_2^i \right], \\ b_3^{\text{EW}} &= \frac{C_F}{N_c^2} \left[C_9 A_1^i + C_7 (A_3^i + A_3^f) + N_c C_8 A_3^f \right], \\ b_4^{\text{EW}} &= \frac{C_F}{N_c^2} \left[C_{10} A_1^i + C_8 A_2^i \right] \end{aligned} \quad (81)$$

and correspond to current–current annihilation (b_1, b_2), penguin annihilation (b_3, b_4), and electroweak penguin annihilation ($b_3^{\text{EW}}, b_4^{\text{EW}}$). These coefficients depend on the final-state mesons, $b_i = b_i(V_1 V_2)$, but this dependence will be left implicit in the following. Finally, the $A_k^{i,f}$ read

$$\begin{aligned}
A_1^i &= \pi\alpha_s \int_0^1 dx dy \left\{ \phi_{\parallel}^{V_1}(y)\phi_{\parallel}^{V_2}(x) \left[\frac{1}{y(1-\bar{y}x)} + \frac{1}{y\bar{x}^2} \right] - \Phi_v^{V_1}(y)\Phi_v^{V_2}(x)r_{\perp}^{V_1}r_{\perp}^{V_2} \frac{2}{y\bar{x}} \right\}, \\
A_1^f &= 0, \\
A_2^i &= \pi\alpha_s \int_0^1 dx dy \left\{ \phi_{\parallel}^{V_1}(y)\phi_{\parallel}^{V_2}(x) \left[\frac{1}{\bar{x}(1-\bar{y}x)} + \frac{1}{y^2\bar{x}} \right] - \Phi_v^{V_1}(y)\Phi_v^{V_2}(x)r_{\perp}^{V_1}r_{\perp}^{V_2} \frac{2}{y\bar{x}} \right\}, \\
A_2^f &= 0, \\
A_3^i &= \pi\alpha_s \int_0^1 dx dy \left\{ \phi_{\parallel}^{V_1}(y)\Phi_v^{V_2}(x)r_{\perp}^{V_2} \frac{2x}{y\bar{x}(1-\bar{y}x)} + \phi_{\parallel}^{V_2}(x)\Phi_v^{V_1}(y)r_{\perp}^{V_1} \frac{2\bar{y}}{y\bar{x}(1-\bar{y}x)} \right\}, \\
A_3^f &= \pi\alpha_s \int_0^1 dx dy \left\{ -\phi_{\parallel}^{V_1}(y)\Phi_v^{V_2}(x)r_{\perp}^{V_2} \frac{2(1+y)}{y^2\bar{x}} + \phi_{\parallel}^{V_2}(x)\Phi_v^{V_1}(y)r_{\perp}^{V_1} \frac{2(1+\bar{x})}{y\bar{x}^2} \right\} \quad (82)
\end{aligned}$$

The superscript i (f) denotes gluon emission from the initial- (final-)state quarks, as shown in Fig. 4 (c) and (d) ((a) and (b)). The subscript k indicates the Dirac structure of the four-quark operators, $\Gamma_1 \otimes \Gamma_2 = (V - A) \otimes (V - A)$ ($k = 1$), $(V - A) \otimes (V + A)$ ($k = 2$), $(-2)(S - P) \otimes (S + P)$ ($k = 3$). The various quantities in (81) will be evaluated at the scale $\mu_h = \sqrt{\Lambda_h} \mu$, similarly to the spectator-interaction terms.

For the numerical estimate of weak annihilation the IR-divergent quantities $A_k^{i,f}$ in (82) will be parametrized by

$$X_A = \int_0^1 \frac{dx}{x} = (1 + \rho_A e^{i\phi_A}) \ln \frac{m_B}{\Lambda_h} \quad (83)$$

The quantity X_A is the cut-off regulated integral $\int_{\Lambda_h/m_B}^1 dx/x = \ln(m_B/\Lambda_h)$, with scale $\Lambda_h = 0.5 \text{ GeV}$, modified by a phenomenological magnitude ρ_A and phase ϕ_A [6]. Using $SU(3)$ flavour symmetry and the asymptotic forms of the meson wavefunctions ϕ_{\parallel} and Φ_v , one finds $A_1^i = A_2^i, A_3^i = 0$ and

$$\begin{aligned}
A_1^i &\approx \pi\alpha_s \left[18 \left(X_A - 4 + \frac{\pi^2}{3} \right) + 18(r_{\perp}^V)^2 (X_A - 2)^2 \right] \\
A_3^f &\approx -36\pi\alpha_s r_{\perp}^V (2X_A^2 - 5X_A + 2) \quad (84)
\end{aligned}$$

We next give the results for the annihilation amplitudes in terms of the coefficients b_i , where we define

$$B_{V_1 V_2} = i \frac{G_F}{\sqrt{2}} f_B f_{V_1} f_{V_2} \quad (85)$$

The decay constant f_B depends on the flavour of the decaying B meson, even though this is not made explicit in the notation for the $B_{V_1 V_2}$. The following expressions can be efficiently obtained with a procedure similar to the one described at the beginning of sec. 3.2. Typical numerical values for the coefficients b_i are given in appendix B. For the channels with $\Delta S = 0$ the annihilation contributions read

$$\mathcal{A}_{\text{ann}}(B^- \rightarrow \rho^- \rho^0) = 0 \quad (86)$$

$$\sqrt{2}\mathcal{A}_{\text{ann}}(B^- \rightarrow \rho^- \omega) = [\lambda_u 2b_2 + (\lambda_u + \lambda_c) 2(b_3 + b_3^{\text{EW}})] B_{\rho\omega} \quad (87)$$

$$\mathcal{A}_{\text{ann}}(B^- \rightarrow \rho^- \phi) = 0 \quad (88)$$

$$\mathcal{A}_{\text{ann}}(B^- \rightarrow K^{*-} K^{*0}) = [\lambda_u b_2 + (\lambda_u + \lambda_c) (b_3 + b_3^{\text{EW}})] B_{K^* K^*} \quad (89)$$

$$\mathcal{A}_{\text{ann}}(\bar{B}_d \rightarrow \rho^0 \rho^0) = \left[\lambda_u b_1 + (\lambda_u + \lambda_c) \left(b_3 + 2b_4 - \frac{1}{2}b_3^{\text{EW}} + \frac{1}{2}b_4^{\text{EW}} \right) \right] B_{\rho\rho} \quad (90)$$

$$\mathcal{A}_{\text{ann}}(\bar{B}_d \rightarrow \rho^0 \omega) = \left[\lambda_u b_1 + (\lambda_u + \lambda_c) \left(-b_3 + \frac{1}{2}b_3^{\text{EW}} + \frac{3}{2}b_4^{\text{EW}} \right) \right] B_{\rho\omega} \quad (91)$$

$$\mathcal{A}_{\text{ann}}(\bar{B}_d \rightarrow \omega\omega) = \left[\lambda_u b_1 + (\lambda_u + \lambda_c) \left(b_3 + 2b_4 - \frac{1}{2}b_3^{\text{EW}} + \frac{1}{2}b_4^{\text{EW}} \right) \right] B_{\omega\omega} \quad (92)$$

$$\mathcal{A}_{\text{ann}}(\bar{B}_d \rightarrow \rho^0 \phi) = 0 \quad (93)$$

$$\mathcal{A}_{\text{ann}}(\bar{B}_d \rightarrow \omega\phi) = 0 \quad (94)$$

$$\mathcal{A}_{\text{ann}}(\bar{B}_d \rightarrow \rho^+ \rho^-) = \left[\lambda_u b_1 + (\lambda_u + \lambda_c) \left(b_3 + 2b_4 - \frac{1}{2}b_3^{\text{EW}} + \frac{1}{2}b_4^{\text{EW}} \right) \right] B_{\rho\rho} \quad (95)$$

$$\mathcal{A}_{\text{ann}}(\bar{B}_d \rightarrow \bar{K}^{*0} K^{*0}) = (\lambda_u + \lambda_c) \left(b_3 + 2b_4 - \frac{1}{2}b_3^{\text{EW}} - b_4^{\text{EW}} \right) B_{K^* K^*} \quad (96)$$

$$\sqrt{2}\mathcal{A}_{\text{ann}}(\bar{B}_s \rightarrow K^{*0} \rho^0) = (\lambda_u + \lambda_c) \left(-b_3 + \frac{1}{2}b_3^{\text{EW}} \right) B_{K^* \rho} \quad (97)$$

$$\sqrt{2}\mathcal{A}_{\text{ann}}(\bar{B}_s \rightarrow K^{*0} \omega) = (\lambda_u + \lambda_c) \left(b_3 - \frac{1}{2}b_3^{\text{EW}} \right) B_{K^* \omega} \quad (98)$$

$$\mathcal{A}_{\text{ann}}(\bar{B}_s \rightarrow K^{*0} \phi) = (\lambda_u + \lambda_c) \left(b_3 - \frac{1}{2}b_3^{\text{EW}} \right) B_{K^* \phi} \quad (99)$$

$$\mathcal{A}_{\text{ann}}(\bar{B}_s \rightarrow K^{*+} \rho^-) = (\lambda_u + \lambda_c) \left(b_3 - \frac{1}{2}b_3^{\text{EW}} \right) B_{K^* \rho} \quad (100)$$

In addition there are two $\Delta S = 0$ decay modes that proceed only through annihilation diagrams:

$$\mathcal{A}_{\text{ann}}(\bar{B}_d \rightarrow K^{*+} K^{*-}) = \left[\lambda_u b_1 + (\lambda_u + \lambda_c) \left(2b_4 + \frac{1}{2}b_4^{\text{EW}} \right) \right] B_{K^* K^*} \quad (101)$$

$$\mathcal{A}_{\text{ann}}(\bar{B}_d \rightarrow \phi\phi) = (\lambda_u + \lambda_c) (2b_4 - b_4^{\text{EW}}) B_{\phi\phi} \quad (102)$$

For the annihilation amplitudes with $\Delta S = 1$ we obtain:

$$\sqrt{2}\mathcal{A}_{\text{ann}}(B^- \rightarrow K^{*-}\rho^0) = [\lambda'_u b_2 + (\lambda'_u + \lambda'_c) (b_3 + b_3^{\text{EW}})] B_{K^*\rho} \quad (103)$$

$$\sqrt{2}\mathcal{A}_{\text{ann}}(B^- \rightarrow K^{*-}\omega) = [\lambda'_u b_2 + (\lambda'_u + \lambda'_c) (b_3 + b_3^{\text{EW}})] B_{K^*\omega} \quad (104)$$

$$\mathcal{A}_{\text{ann}}(B^- \rightarrow K^{*-}\phi) = [\lambda'_u b_2 + (\lambda'_u + \lambda'_c) (b_3 + b_3^{\text{EW}})] B_{K^*\phi} \quad (105)$$

$$\mathcal{A}_{\text{ann}}(B^- \rightarrow \bar{K}^{*0}\rho^-) = [\lambda'_u b_2 + (\lambda'_u + \lambda'_c) (b_3 + b_3^{\text{EW}})] B_{K^*\rho} \quad (106)$$

$$\sqrt{2}\mathcal{A}_{\text{ann}}(\bar{B}_d \rightarrow \bar{K}^{*0}\rho^0) = (\lambda'_u + \lambda'_c) \left(-b_3 + \frac{1}{2}b_3^{\text{EW}} \right) B_{K^*\rho} \quad (107)$$

$$\sqrt{2}\mathcal{A}_{\text{ann}}(\bar{B}_d \rightarrow \bar{K}^{*0}\omega) = (\lambda'_u + \lambda'_c) \left(b_3 - \frac{1}{2}b_3^{\text{EW}} \right) B_{K^*\omega} \quad (108)$$

$$\mathcal{A}_{\text{ann}}(\bar{B}_d \rightarrow \bar{K}^{*0}\phi) = (\lambda'_u + \lambda'_c) \left(b_3 - \frac{1}{2}b_3^{\text{EW}} \right) B_{K^*\phi} \quad (109)$$

$$\mathcal{A}_{\text{ann}}(\bar{B}_d \rightarrow K^{*-}\rho^+) = (\lambda'_u + \lambda'_c) \left(b_3 - \frac{1}{2}b_3^{\text{EW}} \right) B_{K^*\rho} \quad (110)$$

$$\mathcal{A}_{\text{ann}}(\bar{B}_s \rightarrow \rho^0\phi) = 0 \quad (111)$$

$$\mathcal{A}_{\text{ann}}(\bar{B}_s \rightarrow \omega\phi) = 0 \quad (112)$$

$$\mathcal{A}_{\text{ann}}(\bar{B}_s \rightarrow \phi\phi) = (\lambda'_u + \lambda'_c) (2b_3 + 2b_4 - b_3^{\text{EW}} - b_4^{\text{EW}}) B_{\phi\phi} \quad (113)$$

$$\mathcal{A}_{\text{ann}}(\bar{B}_s \rightarrow K^{*+}K^{*-}) = \left[\lambda'_u b_1 + (\lambda'_u + \lambda'_c) \left(b_3 + 2b_4 - \frac{1}{2}b_3^{\text{EW}} + \frac{1}{2}b_4^{\text{EW}} \right) \right] B_{K^*K^*} \quad (114)$$

$$\mathcal{A}_{\text{ann}}(\bar{B}_s \rightarrow \bar{K}^{*0}K^{*0}) = (\lambda'_u + \lambda'_c) \left(b_3 + 2b_4 - \frac{1}{2}b_3^{\text{EW}} - b_4^{\text{EW}} \right) B_{K^*K^*} \quad (115)$$

In the case of $\Delta S = 1$ transitions there are four pure annihilation modes. Their amplitudes have the form:

$$\mathcal{A}_{\text{ann}}(\bar{B}_s \rightarrow \rho^+\rho^-) = \left[\lambda'_u b_1 + (\lambda'_u + \lambda'_c) \left(2b_4 + \frac{1}{2}b_4^{\text{EW}} \right) \right] B_{\rho\rho} \quad (116)$$

$$\mathcal{A}_{\text{ann}}(\bar{B}_s \rightarrow \rho^0\rho^0) = \left[\lambda'_u b_1 + (\lambda'_u + \lambda'_c) \left(2b_4 + \frac{1}{2}b_4^{\text{EW}} \right) \right] B_{\rho\rho} \quad (117)$$

$$\mathcal{A}_{\text{ann}}(\bar{B}_s \rightarrow \omega\omega) = \left[\lambda'_u b_1 + (\lambda'_u + \lambda'_c) \left(2b_4 + \frac{1}{2}b_4^{\text{EW}} \right) \right] B_{\omega\omega} \quad (118)$$

$$\mathcal{A}_{\text{ann}}(\bar{B}_s \rightarrow \rho^0\omega) = \left[\lambda'_u b_1 + (\lambda'_u + \lambda'_c) \frac{3}{2}b_4^{\text{EW}} \right] B_{\rho\omega} \quad (119)$$

Table 1: Experimental results [24] for CP-averaged branching ratios and longitudinal polarization fractions f_L of $\bar{B} \rightarrow VV$ decays. Here the B meson is either a B^- or a \bar{B}_d . The branching ratios for $\bar{B} \rightarrow V_L V_L$ have been obtained as $f_L B(\bar{B} \rightarrow VV)$. Also shown are the direct CP asymmetries $A_{CP} \equiv -C \equiv (B(\bar{B} \rightarrow \bar{f}) - B(B \rightarrow f))/(B(\bar{B} \rightarrow \bar{f}) + B(B \rightarrow f))$. The label (L) indicates that A_{CP} refers to vector mesons with longitudinal polarization only.

VV	$B(\bar{B} \rightarrow VV)/10^{-6}$	f_L	$B(\bar{B} \rightarrow V_L V_L)/10^{-6}$	A_{CP}
$\rho^+ \rho^-$	$24.2^{+3.1}_{-3.2}$	$0.978^{+0.025}_{-0.022}$	23.7 ± 3.2	0.06 ± 0.13 (L)
$\rho^0 \rho^0$	0.68 ± 0.27	0.70 ± 0.15	0.48 ± 0.21	-0.4 ± 0.9 (L)
$\rho^- \rho^0$	18.2 ± 3.0	$0.912^{+0.044}_{-0.045}$	16.6 ± 2.9	-0.08 ± 0.13
$\rho^- \omega$	$10.6^{+2.6}_{-2.3}$	0.82 ± 0.11	8.7 ± 2.4	0.04 ± 0.18
$\bar{K}^{*0} K^{*0}$	$1.28^{+0.37}_{-0.32}$ [25]	$0.80^{+0.12}_{-0.13}$ [25]	1.02 ± 0.32	—
$\bar{K}^{*0} \rho^0$	5.6 ± 1.6	0.57 ± 0.12	3.2 ± 1.1	0.09 ± 0.19
$K^{*-} \rho^+$	< 12	—	< 12	—
$K^{*-} \rho^0$	< 6.1	$0.96^{+0.06}_{-0.16}$	< 6.1	$0.20^{+0.32}_{-0.29}$
$\bar{K}^{*0} \rho^-$	9.2 ± 1.5	0.48 ± 0.08	4.4 ± 1.0	-0.01 ± 0.16
$\bar{K}^{*0} \phi$	9.5 ± 0.8	0.484 ± 0.034	4.6 ± 0.5	-0.01 ± 0.06
$K^{*-} \phi$	10.0 ± 1.1	0.50 ± 0.05	5.0 ± 0.7	-0.01 ± 0.08
$\bar{K}^{*0} \omega$	$1.8^{+0.8}_{-0.7}$ [26]	$0.56^{+0.34}_{-0.30}$ [26]	1.0 ± 0.7	—

Because of similarities in the flavour structure of $\mathcal{T}_p^{d(s)}$ and $\mathcal{T}_p^{ann,d(s)}$, in all amplitudes the coefficient b_3 appears together with the factorization coefficient a_4^p in the combination $a_4^p + B_{V_1 V_2}/A_{V_1 V_2} b_3$. This has been noted before in the context of PP and PV final states [23].

4 Experimental results and input parameters

Available data on the decays of B^- and \bar{B}_d mesons into a pair of light vector mesons are displayed in Tables 1 and 2. The results are from [24] unless indicated otherwise. CP averaging is understood for branching ratios and f_L . No data are available yet on $\bar{B}_s \rightarrow VV$ decays.

Table 3 collects the input parameters used in our analysis. The values of m_V , Γ_V , m_B , $|V_{us}|$ and $|V_{cb}|$ have been taken from [28]. They have only small uncertainties, which we neglect. Our choice for $|V_{ub}/V_{cb}|$ is compatible with the exclusive determinations quoted in [28]. We prefer those over the inclusive values since we use V_{ub} in exclusive

Table 2: Experimental results for further $B \rightarrow VV$ decays [24]. Quoted are the CP-averaged branching fractions in units of 10^{-6} . The B meson is either a B^- or a \bar{B}_d .

$K^{*-}\omega$	$K^{*-}K^{*0}$	$\rho^-\phi$ [27]	$\bar{K}^{*0}\omega$	$K^{*+}K^{*-}$
< 3.4	< 71	< 3	< 2.7	< 141
$\rho^0\omega$	$\omega\omega$	$\rho^0\phi$ [27]	$\omega\phi$	$\phi\phi$ [27]
< 1.5	< 4.0	< 0.33	< 1.2	< 0.2

processes where the form factors rely on similar theoretical methods (light-cone QCD sum rules, lattice) as in the exclusive extraction of $|V_{ub}|$. The lifetimes of B^- and \bar{B}_d are also from [28]. On the other hand, the lifetime of \bar{B}_s is put equal to $\tau_{\bar{B}_d}$, which is expected theoretically to hold to very high accuracy. The value of $\tau_{\bar{B}_s}$ from [28] is compatible with this, but is still affected by a larger error.

The number for $\sin 2\beta$ is the average of [24] from CP violation in $b \rightarrow c\bar{c}s$ modes. The angle γ corresponds to the result of global CKM fits [29,30]. The standard model parameters $\Lambda_{\overline{\text{MS}}}^{(5)}$, m_b , m_c , m_t and M_W are the same as in [6]. Changes in these values have been small in comparison with the relevant uncertainties. The quark masses are running $\overline{\text{MS}}$ -masses.

The decay constants f_V can be determined from data on $V \rightarrow l^+l^-$ and $\tau \rightarrow V\nu$. We use the values quoted in [23]. The transverse decay constants f_V^\perp need to be computed theoretically, for instance with QCD sum rules. The results we use for f_V^\perp have been compiled in [31]. The $B \rightarrow V$ form factors are from QCD sum rules on the light cone [32]. These results do not yet incorporate some improvements in the treatment of $SU(3)$ breaking that has been achieved in the meantime (see comments in sec. 2.3 of [1]). The uncertainties on the form factors in Table 3 are taken to be somewhat larger than reported in [32]. The Gegenbauer coefficients $\alpha_{1,2}^V$ are still rather uncertain. We adopt numbers of the typical size found in QCD sum rule calculations [32], [33] and allow for sizable uncertainties. The range of numbers for the B -meson decay constants is representative of results from recent unquenched lattice simulations (see sec. 2.4 in [1] for a review and detailed references). The parameter λ_B is not well known at present. We shall consider here the generous range already used in [6]. No attempt is made to account for $SU(3)$ breaking in this quantity.

Table 3: Input parameters for $B \rightarrow V_L V_L$ decays. Here B_q stands for either B^- or \bar{B}_d . The values of the scale dependent quantities $f_V^\perp = f_V^\perp(\mu)$ are given for $\mu = 1$ GeV. The scale dependence of $\alpha_{1,2}^V$ is neglected.

Light vector mesons						
V	m_V/MeV	Γ_V/MeV	f_V/MeV	f_V^\perp/MeV	α_1^V	α_2^V
ρ	776	149	209	165 ± 9	0	0.1 ± 0.3
ω	783	8	187	151 ± 9	0	0.1 ± 0.3
K^*	894	51	218	185 ± 10	0.1 ± 0.1	0.1 ± 0.3
ϕ	1019	4	221	186 ± 9	0	0.1 ± 0.3
B mesons						
B	m_B/GeV	τ_B/ps	f_B/MeV	λ_B/MeV		
B^-	5.28	1.64	200 ± 30	350 ± 150		
\bar{B}_d	5.28	1.53	200 ± 30	350 ± 150		
\bar{B}_s	5.37	1.53	230 ± 30	350 ± 150		
Form factors						
$A_0^{B_q \rightarrow \rho}(0)$	$A_0^{B_q \rightarrow \omega}(0)$	$A_0^{B_q \rightarrow K^*}(0)$	$A_0^{B_s \rightarrow K^*}(0)$	$A_0^{B_s \rightarrow \phi}(0)$		
0.30 ± 0.04	0.28 ± 0.05	0.37 ± 0.05	0.36 ± 0.05	0.47 ± 0.06		
SM parameters						
$\Lambda_{\overline{\text{MS}}}^{(5)}/\text{MeV}$	$m_b(m_b)/\text{GeV}$	$m_c(m_b)/\text{GeV}$	$m_t(m_t)/\text{GeV}$	M_W/GeV		
225	4.2	1.3 ± 0.2	167	80.4		
$ V_{us} $	$ V_{cb} $	$ V_{ub}/V_{cb} $	γ	$\sin 2\beta$		
0.226	0.0416	0.09 ± 0.01	$(67 \pm 12)^\circ$	0.681 ± 0.025		

5 Phenomenological analysis

5.1 $B \rightarrow V_L V_L$ branching fractions

The branching fraction of a decay $\bar{B} \rightarrow V_{1L} V_{2L}$ is obtained from the corresponding amplitude \mathcal{A} as

$$B(\bar{B} \rightarrow V_{1L} V_{2L}) = S \frac{\tau_B}{16\pi m_B} |\mathcal{A}(\bar{B} \rightarrow V_{1L} V_{2L})|^2 \quad (120)$$

Here S is a symmetry factor with $S = 1/2$ if V_1 and V_2 are identical and $S = 1$ otherwise.

Predictions of CP averaged branching ratios are compiled in Table 4 and Table 5 for strangeness-conserving and strangeness-changing $\bar{B} \rightarrow V_{1L} V_{2L}$ decays, respectively. Absolute branching fractions have in general sizable uncertainties from hadronic input quantities, for instance from $B \rightarrow V_L$ form factors. Taking ratios or other combinations

Table 4: CP-averaged branching fractions for $B \rightarrow V_L V_L$ decays with $\Delta S = 0$. The sensitivity to variations in the input parameters according to Table 3 is displayed where the upper (lower) entry corresponds to the larger (smaller) value of the parameter. The renormalization scale μ is varied between $2m_b$ and $m_b/2$. The model parameters $X_{A,H}(\rho_{A,H}, \phi_{A,H})$ from power corrections are varied within the range given by $0 \leq \rho_{A,H} \leq 1$ and $0 \leq \phi_{A,H} \leq 2\pi$. Here upper (lower) entries refer to positive (negative) $\text{Im}X_{A,H}$. The appropriate units for each mode are given in square brackets.

mode	central	A_0	α_2^V	λ_B	f_B	μ	X_A	X_H	$\frac{V_{ub}}{V_{cb}}$	γ
$B^- \rightarrow \rho^- \rho^0$	17.5[10 ⁻⁶]	+4.5 -4.0	+1.9 -1.4	-0.9 +2.5	+0.5 -0.5	+0.1 -0.0	—	+1.5 -1.4	+4.1 -3.6	-0.2 +0.2
$B^- \rightarrow \rho^- \omega$	15.5[10 ⁻⁶]	+5.6 -4.7	+1.4 -0.9	-0.8 +2.0	+0.3 -0.3	+0.3 -0.3	-1.2 +0.9	+1.2 -1.1	+3.4 -3.0	-0.8 +0.7
$B^- \rightarrow \rho^- \phi$	6.0[10 ⁻⁹]	+0.9 -0.8	+3.7 -2.2	-1.5 +4.8	+0.9 -0.8	-1.1 +3.4	—	+2.8 -2.2	+0.0 -0.0	+1.1 -1.0
$B^- \rightarrow K^{*-} K^{*0}$	2.7[10 ⁻⁷]	+0.9 -0.8	-0.8 +0.9	+0.2 -0.4	-0.1 +0.1	-0.4 +0.5	-2.5 +3.9	-0.3 +0.3	+0.0 -0.0	+0.5 -0.5
$\bar{B}_d \rightarrow \rho^0 \rho^0$	3.3[10 ⁻⁷]	+0.3 -0.3	+4.3 -1.6	-1.3 +6.1	+0.7 -0.6	-0.0 +0.7	+2.2 -1.7	-2.2 +3.7	+0.8 -0.7	+0.3 -0.3
$\bar{B}_d \rightarrow \rho^0 \omega$	8.0[10 ⁻⁸]	+3.1 -2.5	-3.3 +3.9	+1.1 -2.4	-0.4 +0.5	-1.4 +1.4	-2.7 +22.5	-1.6 +1.8	+0.4 -0.3	+2.3 -2.1
$\bar{B}_d \rightarrow \omega \omega$	5.0[10 ⁻⁷]	+0.7 -0.6	+3.7 -1.7	-1.4 +5.4	+1.0 -0.9	-0.2 +1.0	-1.3 +2.1	-2.3 +3.3	+0.9 -0.8	-0.4 +0.4
$\bar{B}_d \rightarrow \rho^0 \phi$	2.8[10 ⁻⁹]	+0.4 -0.4	+1.7 -1.0	-0.7 +2.2	+0.4 -0.4	-0.5 +1.6	—	-1.0 +1.3	+0.0 -0.0	+0.5 -0.5
$\bar{B}_d \rightarrow \omega \phi$	2.4[10 ⁻⁹]	+0.5 -0.4	+1.4 -0.9	-0.6 +1.8	+0.3 -0.3	-0.4 +1.2	—	-0.9 +1.1	+0.0 -0.0	+0.4 -0.4
$\bar{B}_d \rightarrow \rho^+ \rho^-$	25.8[10 ⁻⁶]	+7.6 -6.6	-2.0 +1.6	+1.0 -2.4	-0.3 +0.3	-0.3 +0.1	+2.4 -1.8	-1.5 +1.5	+5.8 -5.2	-0.9 +0.8
$\bar{B}_d \rightarrow \bar{K}^{*0} K^{*0}$	3.2[10 ⁻⁷]	+0.9 -0.8	-0.9 +0.9	+0.2 -0.4	+0.0 -0.0	-0.7 +0.9	-2.5 +3.0	-0.3 +0.4	+0.0 -0.0	+0.5 -0.4
$\bar{B}_s \rightarrow K^{*0} \rho^0$	5.6[10 ⁻⁷]	+0.4 -0.4	+6.7 -2.7	-2.1 +8.8	+1.2 -1.0	-0.0 +1.1	-0.4 +1.5	-4.2 +7.5	+1.3 -1.2	+0.4 -0.4
$\bar{B}_s \rightarrow K^{*0} \omega$	6.5[10 ⁻⁷]	+0.9 -0.7	+5.5 -2.3	-1.9 +7.6	+1.0 -0.9	-0.0 +0.9	-0.9 +1.6	-3.9 +6.6	+1.2 -1.1	-0.5 +0.4
$\bar{B}_s \rightarrow K^{*0} \phi$	3.4[10 ⁻⁷]	+1.1 -1.0	-1.3 +1.4	+0.3 -0.7	-0.2 +0.2	-0.6 +0.6	-3.3 +5.1	-0.7 +0.8	-0.0 +0.0	+0.5 -0.5
$\bar{B}_s \rightarrow K^{*+} \rho^-$	37.2[10 ⁻⁶]	+11.8 -10.2	-2.9 +2.3	+1.4 -3.3	-0.6 +0.6	+0.0 -0.3	-0.2 +0.4	-2.6 +2.7	+8.4 -7.5	-1.2 +1.1
$\bar{B}_d \rightarrow K^{*+} K^{*-}$	2.9[10 ⁻⁸]	—	—	—	+0.9 -0.8	-1.0 +2.2	-2.8 +19.1	—	+0.5 -0.4	-0.4 +0.3
$\bar{B}_d \rightarrow \phi \phi$	2.5[10 ⁻⁹]	—	—	—	+0.8 -0.7	-1.3 +3.4	+16.7 -2.4	—	+0.0 -0.0	+0.5 -0.4

Table 5: CP-averaged branching fractions for $B \rightarrow V_L V_L$ decays with $\Delta S = 1$. The sensitivity to variations in the input parameters according to Table 3 is displayed where the upper (lower) entry corresponds to the larger (smaller) value of the parameter. The renormalization scale μ is varied between $2m_b$ and $m_b/2$. The model parameters $X_{A,H}(\rho_{A,H}, \phi_{A,H})$ from power corrections are varied within the range given by $0 \leq \rho_{A,H} \leq 1$ and $0 \leq \phi_{A,H} \leq 2\pi$. Here upper (lower) entries refer to positive (negative) $\text{Im}X_{A,H}$. The appropriate units for each mode are given in square brackets.

mode	central	A_0	α_1^V	α_2^V	λ_B	f_B	μ	X_A	X_H	γ
$B^- \rightarrow K^{*-} \rho^0$	3.4[10 ⁻⁶]	+1.0 -0.9	-0.1 +0.1	-0.6 +0.7	+0.1 -0.2	-0.1 +0.1	-0.2 +0.1	-2.5 +3.7	-0.1 +0.1	+0.7 -0.7
$B^- \rightarrow K^{*-} \omega$	1.7[10 ⁻⁶]	+0.8 -0.6	-0.1 +0.1	-0.4 +0.6	+0.2 -0.3	-0.1 +0.1	-0.1 +0.0	-1.0 +2.4	-0.2 +0.3	+0.5 -0.4
$B^- \rightarrow K^{*-} \phi$	4.1[10 ⁻⁶]	+1.5 -1.3	-0.1 +0.1	-1.7 +2.0	+0.5 -1.2	-0.3 +0.3	-0.7 +0.5	-4.1 +7.8	-0.9 +1.0	-0.0 +0.0
$B^- \rightarrow \bar{K}^{*0} \rho^-$	3.3[10 ⁻⁶]	+1.1 -1.0	-0.3 +0.3	-1.1 +1.2	+0.3 -0.6	-0.2 +0.2	-0.4 +0.3	-3.3 +6.5	-0.4 +0.4	-0.0 +0.0
$\bar{B}_d \rightarrow \bar{K}^{*0} \rho^0$	5.0[10 ⁻⁷]	+1.7 -1.4	-0.6 +0.6	-1.7 +2.5	+0.2 -0.2	-0.3 +0.3	-1.1 +0.9	-4.7 +24.2	-0.2 +0.3	-0.2 +0.2
$\bar{B}_d \rightarrow \bar{K}^{*0} \omega$	1.4[10 ⁻⁶]	+0.8 -0.6	-0.2 +0.2	-0.7 +0.8	+0.3 -0.6	-0.2 +0.2	-0.1 +0.0	-1.3 +2.7	-0.4 +0.5	+0.0 -0.0
$\bar{B}_d \rightarrow \bar{K}^{*0} \phi$	3.7[10 ⁻⁶]	+1.4 -1.2	-0.1 +0.1	-1.6 +1.8	+0.5 -1.1	-0.3 +0.3	-0.6 +0.4	-3.7 +7.5	+0.9 -0.8	-0.0 +0.0
$\bar{B}_d \rightarrow K^{*-} \rho^+$	3.0[10 ⁻⁶]	+1.0 -0.8	-0.2 +0.2	-0.7 +0.8	+0.1 -0.3	-0.1 +0.1	-0.3 +0.2	-1.8 +5.4	-0.1 +0.1	+0.8 -0.7
$\bar{B}_s \rightarrow \rho^0 \phi$	5.9[10 ⁻⁷]	+1.8 -1.5	—	-0.5 +0.5	+0.4 -0.6	-0.1 +0.1	+0.1 -0.0	—	-0.6 +0.9	+0.5 -0.4
$\bar{B}_s \rightarrow \omega \phi$	4.4[10 ⁻⁸]	+1.3 -0.7	—	+5.1 -0.0	-0.0 +8.4	+0.4 -0.0	-0.1 +4.0	—	-1.8 +11.3	+0.5 -0.4
$\bar{B}_s \rightarrow \phi \phi$	15.5[10 ⁻⁶]	+5.0 -4.3	—	-5.8 +6.5	+1.6 -3.6	-0.7 +0.7	-3.1 +3.3	-14.4 +20.2	-3.2 +3.6	-0.1 +0.1
$\bar{B}_s \rightarrow K^{*+} K^{*-}$	5.9[10 ⁻⁶]	+1.7 -1.5	-0.3 +0.3	-1.3 +1.4	+0.2 -0.4	+0.0 -0.0	-0.9 +1.1	-3.8 +6.5	-0.3 +0.3	+1.5 -1.3
$\bar{B}_s \rightarrow \bar{K}^{*0} K^{*0}$	6.2[10 ⁻⁶]	+1.9 -1.7	-0.3 +0.3	-1.9 +2.0	+0.4 -1.0	-0.1 +0.1	-1.2 +1.5	-5.6 +7.5	-0.7 +0.7	-0.0 +0.0
$\bar{B}_s \rightarrow \rho^+ \rho^-$	1.0[10 ⁻⁷]	—	—	—	—	+0.3 -0.2	-0.5 +1.4	+6.7 -1.0	—	+0.0 -0.0
$\bar{B}_s \rightarrow \rho^0 \rho^0$	5.1[10 ⁻⁸]	—	—	—	—	+1.4 -1.2	-2.7 +7.0	+33.7 -5.0	—	+0.2 -0.2
$\bar{B}_s \rightarrow \omega \omega$	3.2[10 ⁻⁸]	—	—	—	—	+0.9 -0.8	-1.7 +4.5	-3.2 +21.6	—	+0.1 -0.1
$\bar{B}_s \rightarrow \rho^0 \omega$	1.5[10 ⁻⁹]	—	—	—	—	+0.4 -0.4	-0.5 +1.1	+9.8 -1.4	—	-0.1 +0.1

of suitable branching fractions can eliminate part of the uncertainties and lead to theoretically cleaner observables. In spite of this it is still interesting to present the theory expectations for the branching fractions, which can be directly confronted with experimental data. In addition, we use Tables 4 and 5 to display in detail the sensitivity of the results on the most important input parameters.

In Fig. 5 we compare theory and experiment for $\bar{B} \rightarrow V_L V_L$ branching fractions, for which measurements are available. For this comparison the form factors have been fixed to their central values. In the present discussion we will assume that the Standard Model is valid. Under this assumption the comparison with experimental data will serve as a test of the theory of QCD interactions in hadronic weak decays. It should be kept in mind that possible deviations between predictions and measurements may in principle indicate the existence of New Physics. In order to disentangle New Physics from QCD effects it is important to consider observables with very little hadronic uncertainty. We will discuss several examples for this in the following sections. For the moment we stay with the discussion of the theoretically less clean absolute branching fractions for the purpose of testing the method of QCD factorization, under the (provisional) assumption that physics beyond the Standard Model is absent.

Fig. 5 shows good agreement of theory and experiment within errors. An exception is $B^- \rightarrow \rho^- \omega$, where the measured branching ratio is somewhat low with respect to the expectation from theory. The reason could be an overestimate of the $B \rightarrow \omega$ form factor, or a statistical fluctuation. The only other measured decay with an ω is $\bar{B}_d \rightarrow \bar{K}^{*0} \omega$. Here the theory result is also above the central experimental value, but the uncertainties in the latter are still larger than for $B^- \rightarrow \rho^- \omega$ and prevent any firm conclusion.

We emphasize that theory and experiment agree very well in the three ρ -meson channels $\bar{B}_d \rightarrow \rho^+ \rho^-$, $\bar{B}_d \rightarrow \rho^0 \rho^0$ and $B^- \rightarrow \rho^- \rho^0$, as it has also been found in [11]. The $\rho^0 \rho^0$ channel is a colour-suppressed mode and comes with large uncertainties. Hard spectator scattering plays an important role and therefore the sensitivity to the poorly known parameter λ_B is large. Still the experimental result can be accounted for naturally with default values of the hadronic parameters. It is remarkable that the observed pattern of all three $\rho\rho$ branching ratios, which exhibit rather different values, is nicely reproduced within QCD factorization. The fact that this works for the central $B \rightarrow \rho$ form factor A_0 supports the numerical value used for this quantity.

The penguin modes $\bar{B}_d \rightarrow \bar{K}^{*0} K^{*0}$ and $\bar{B}_d \rightarrow \bar{K}^{*0} \rho^0$ tend to have relatively small predicted branching ratios, which however stretch into the range of measured values within errors. The compatibility is better for $\bar{B}_d \rightarrow \bar{K}^{*0} K^{*0}$ than for $\bar{B}_d \rightarrow \bar{K}^{*0} \rho^0$. At the same time the latter mode is also seen to be very sensitive to the annihilation contributions.

It is interesting to note that the central values of the experimental and theoretical results are particularly close for the penguin decays $B^- \rightarrow \bar{K}^{*0} \rho^-$, $\bar{B}_d \rightarrow \bar{K}^{*0} \phi$, $B^- \rightarrow K^{*-} \phi$. On the other hand, the dependence on weak annihilation is very strong. The huge variations from these effects shown in Fig. 5 suggest that, at least for these channels, the annihilation model used by us is likely to overestimate the related uncertainty.

Further branching ratio predictions and information on the various error sources for

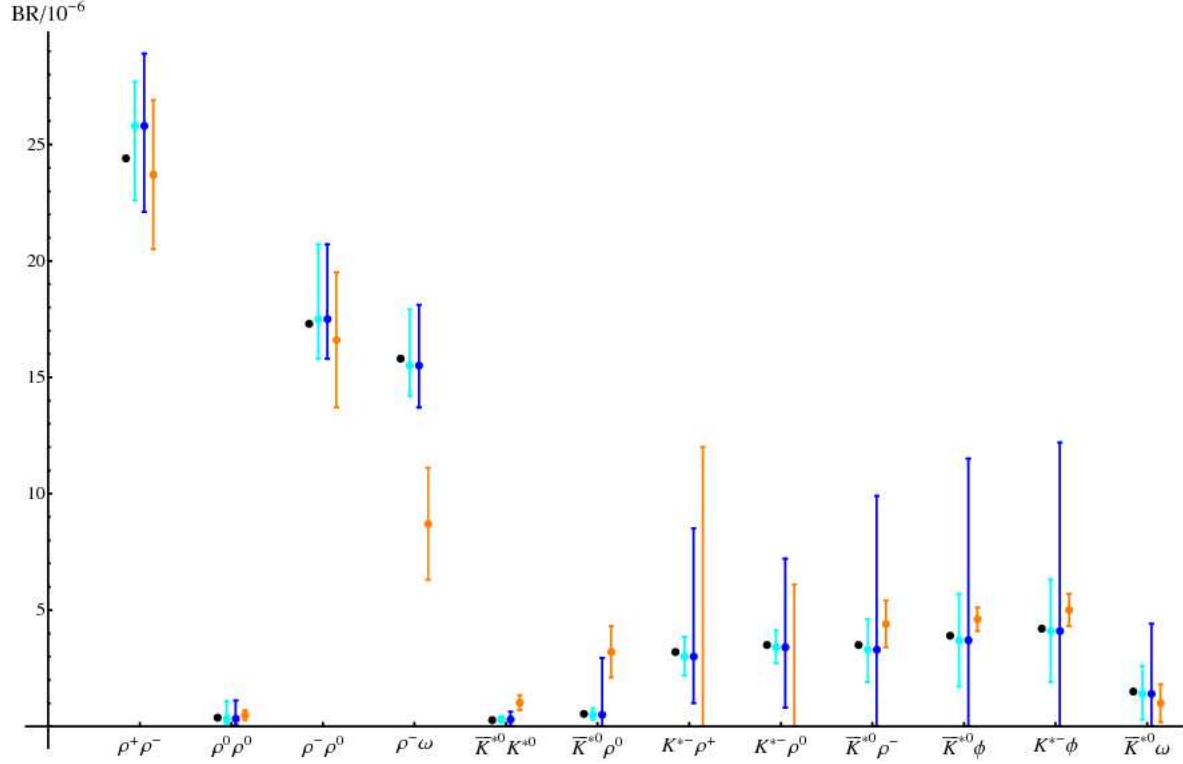


Figure 5: Comparison between theory predictions [dots (black), left bar (cyan), middle bar (marine blue)] and experimental results [right bar (orange)] for $\bar{B}_d \rightarrow V_L V_L$ modes, for which measurements are available. The theoretical error bars display the hadronic errors without [left (cyan)] and with [middle (marine blue)] the model-dependent error estimate for annihilation topologies. The form-factor uncertainties are not included in the error bars. The black dots are the central values of the theory predictions where all power corrections have been omitted. From experiment only upper limits are known for the two $K^{*-}\rho$ channels.

all 34 $\bar{B} \rightarrow V_L V_L$ decays can be obtained from Tables 4 and 5.

Our results include estimates of some effects that are suppressed by a factor of Λ_{QCD}/m_b . These corrections are weak annihilation and the effects proportional to r_{\perp}^V (see eq. (25)). Terms at this order are not calculable in QCD factorization. They have still been included as model estimates in order to permit us to assess the sensitivity of factorization predictions on potentially important power corrections. Weak annihilation is the most prominent example. For the default choice of input parameters the impact of power corrections on the predicted branching ratios is in general small. This can already be seen from Fig. 5, where central results with all power corrections omitted are indicated by the black dots. They differ very little from the central theory predictions that include such effects. To make these statements more quantitative, we list the differences between the central values for all $\Delta S = 0$ branching ratios without and including power corrections, $BR(\text{no power corr.})/BR(\text{default}) - 1$, in the order of appearance in Table 4, in %:

$$-1, +2, -6, +6, +15, +7, -27, -6, -6, -5, -16, -12, -9, +6, +1, -100, -100 \quad (121)$$

The same information for the $\Delta S = 1$ decays of Table 5 reads

$$+5, +5, +3, +7, +9, +12, +6, +7, +2, +0, -8, -17, -19, -100, -100, -100, -100 \quad (122)$$

The deviation is -100% for the six pure annihilation decays, which have no leading-power contribution. In all other cases the impact of the default power corrections is rather moderate or indeed very small, notably for the dominant decay channels.

We finally comment on the impact of the long-distance electromagnetic penguin correction defined in (39) and discussed in appendix A. This contribution affects only decays with the emission of ρ^0 , ω or ϕ , where it enters through the coefficient $a_7^u + a_9^u$. The long-distance effects are sizable, on the scale of this coefficient, for ρ^0 and ω , but much less in the case of ϕ . Since the long-distance terms are of order $\alpha = 1/129$ their overall contribution is in general very small. This is particularly true for the $\Delta S = 1$ decays where the up-quark sector is also CKM suppressed. For the $\Delta S = 0$ transitions the absence of the term in (39) would change branching ratios at the level of a few percent at most and below the size of most of the other uncertainties. The situation is similar for the direct CP asymmetries in the $\Delta S = 0$ modes with the exception of $\rho^-\rho^0$, $\rho^-\phi$, $\rho^0\omega$, $\rho^0\phi$ and $\omega\phi$, where the impact is relatively large. However, in any case, the direct CP asymmetry is very uncertain for $\rho^0\omega$ and it is very small for the remaining channels.

5.2 Direct CP violation in $B \rightarrow V_L V_L$

Direct CP asymmetries require the presence of a strong as well as a weak phase difference between two interfering amplitudes. In the heavy-quark limit this phase difference arises at order α_s . It is therefore parametrically suppressed and at the same time sensitive to uncalculable power corrections. This makes it difficult to obtain accurate predictions for direct CP violation. At present the most precisely measured direct CP asymmetry

in B decays is $A_{CP}(B \rightarrow K^+\pi^-) = -0.097 \pm 0.012$ [24]. The corresponding strong phase difference is small ($\sim 15^\circ$) [34], but has a sign opposite to the $\mathcal{O}(\alpha_s)$ result in the heavy-quark limit. This may indicate the importance of Λ/m_b corrections.

In Tables 6 and 7 we show estimates of direct CP asymmetries for the decays under discussion. The values have large uncertainties, as anticipated. Most of the asymmetries

Table 6: CP asymmetries for $B \rightarrow V_L V_L$ decays with $\Delta S = 0$, defined as $A_{CP} \equiv (B(\bar{B} \rightarrow \bar{f}) - B(B \rightarrow f))/(B(\bar{B} \rightarrow \bar{f}) + B(B \rightarrow f))$. The sensitivity to variations in the input parameters according to Table 3 is displayed where the upper (lower) entry corresponds to the larger (smaller) value of the parameter. The renormalization scale μ is varied between $2m_b$ and $m_b/2$. The model parameters $X_{A,H}(\rho_{A,H}, \phi_{A,H})$ from power corrections are varied within the range given by $0 \leq \rho_{A,H} \leq 1$ and $0 \leq \phi_{A,H} \leq 2\pi$. The appropriate units for each mode are given in square brackets. We refrain from quoting estimates of CP asymmetries for pure annihilation modes.

mode	central	m_c	α_2^V	λ_B	f_B	μ	X_A	X_H	$\frac{V_{ub}}{V_{cb}}$	γ
$B^- \rightarrow \rho^- \rho^0$	$-2.6[10^{-4}]$	+0.8 -0.7	+0.2 -0.3	+0.1 -0.2	-0.0 +0.0	-5.6 +7.4	—	+3.7 -3.7	+0.3 -0.3	-0.2 +0.3
$B^- \rightarrow \rho^- \omega$	$-9.3[10^{-2}]$	+2.4 -2.0	+1.0 -1.0	-0.4 +0.8	+0.2 -0.2	+1.4 -2.2	+22.4 -21.6	+3.1 -3.1	+0.8 -1.0	-1.1 +1.4
$B^- \rightarrow \rho^- \phi$	$-1.2[10^{-2}]$	-0.0 +0.0	+0.2 -0.3	-0.2 +0.3	+0.1 -0.1	-1.1 +1.1	—	+0.2 -0.4	-0.1 +0.1	+0.1 -0.1
$B^- \rightarrow K^{*-} K^{*0}$	$-1.0[10^{-1}]$	-1.0 +0.9	-0.0 +0.1	+0.0 -0.1	+0.1 -0.1	+0.1 -0.2	+8.9 -7.9	+0.1 -0.1	-0.1 +0.1	+0.1 -0.1
$\bar{B}_d \rightarrow \rho^0 \rho^0$	$+5.3[10^{-1}]$	-0.7 +0.4	-2.7 +3.8	+2.2 -2.8	-0.7 +0.8	-1.0 +0.7	+4.3 -5.8	+3.6 -2.8	-0.5 +0.6	-0.2 +0.0
$\bar{B}_d \rightarrow \rho^0 \omega$	$+7.8[10^{-2}]$	-17.4 +14.9	+13.9 -5.3	-2.0 +7.4	+6.7 -6.1	-5.3 +10.8	+92.2 -107.8	+10.2 -10.2	+0.5 -0.6	-1.3 +1.6
$\bar{B}_d \rightarrow \omega \omega$	$-4.5[10^{-1}]$	+0.5 -0.4	+1.9 -2.4	-1.5 +2.1	+0.6 -0.8	+0.7 -0.5	+5.0 -2.7	+2.7 -2.8	+0.3 -0.3	-0.7 +0.8
$\bar{B}_d \rightarrow \rho^0 \phi$	$-1.2[10^{-2}]$	-0.0 +0.0	+0.2 -0.3	-0.2 +0.3	+0.1 -0.1	-1.1 +1.1	—	+0.2 -0.4	-0.1 +0.1	+0.1 -0.1
$\bar{B}_d \rightarrow \omega \phi$	$-1.2[10^{-2}]$	-0.0 +0.0	+0.2 -0.3	-0.2 +0.3	+0.1 -0.1	-1.1 +1.1	—	+0.3 -0.4	-0.1 +0.1	+0.1 -0.1
$\bar{B}_d \rightarrow \rho^+ \rho^-$	$-3.7[10^{-2}]$	+1.4 -1.2	+0.0 -0.0	+0.1 -0.2	-0.0 +0.0	+0.3 -0.3	+10.7 -10.5	+0.2 -0.2	+0.3 -0.4	-0.4 +0.5
$\bar{B}_d \rightarrow \bar{K}^{*0} K^{*0}$	$-1.5[10^{-1}]$	-0.7 +0.6	-0.2 +0.2	+0.0 -0.1	-0.0 +0.0	+0.2 -0.4	+0.9 -2.2	+0.1 -0.1	-0.2 +0.2	+0.1 -0.0
$\bar{B}_s \rightarrow K^{*0} \rho^0$	$+4.3[10^{-1}]$	-0.7 +0.4	-2.1 +3.4	+1.7 -2.1	-0.6 +0.7	-0.7 +0.3	+4.5 -8.2	+4.2 -2.5	-0.4 +0.5	+0.0 -0.2
$\bar{B}_s \rightarrow K^{*0} \omega$	$-5.2[10^{-1}]$	+0.5 -0.4	+2.4 -2.9	-1.7 +2.5	+0.6 -0.7	+0.9 -0.5	+6.7 -3.6	+3.9 -3.7	+0.3 -0.3	-0.8 +0.9
$\bar{B}_s \rightarrow K^{*0} \phi$	$-2.0[10^{-1}]$	-0.8 +0.7	-0.5 +0.3	+0.1 -0.3	-0.1 +0.1	+0.3 -0.7	+2.3 -7.6	+0.3 -0.3	-0.2 +0.2	+0.1 -0.1
$\bar{B}_s \rightarrow K^{*+} \rho^-$	$-3.9[10^{-2}]$	+1.5 -1.2	+0.0 -0.0	+0.1 -0.2	-0.0 +0.0	+0.3 -0.4	+13.6 -13.5	+0.2 -0.2	+0.4 -0.4	-0.4 +0.5

are small or moderate, but there can be exceptions. Large asymmetries may occur when the interfering amplitudes have comparable magnitude and a substantial strong relative phase. Examples are the $\Delta S = 0$ decays with a colour suppressed tree contribution ($\sim a_2$), as $\bar{B}_d \rightarrow \rho^0 \rho^0$, $\omega \omega$ or $\bar{B}_s \rightarrow K^{*0} \rho^0$, $K^{*0} \omega$. Despite the α_s factor the strong phase difference can here be naturally more sizeable. Generically, a decay amplitude of the

Table 7: CP asymmetries for $B \rightarrow V_L V_L$ decays with $\Delta S = 1$ (see caption of Table 6 for details).

mode	central	m_c	α_1^V	α_2^V	λ_B	μ	X_A	X_H	$\frac{V_{ub}}{V_{cb}}$	γ
$B^- \rightarrow K^{*-} \rho^0$	2.9[10 ⁻¹]	-0.7 +0.6	-0.1 +0.1	+0.5 -0.4	-0.1 +0.3	-0.1 +0.3	+7.0 -9.0	+0.8 -0.9	+0.3 -0.3	-0.4 +0.3
$B^- \rightarrow K^{*-} \omega$	4.9[10 ⁻¹]	-1.1 +0.9	-0.0 +0.0	+1.4 -1.1	-0.5 +1.1	-0.5 +1.4	+5.1 -13.3	+1.9 -2.2	+0.2 -0.3	-0.8 +0.9
$B^- \rightarrow K^{*-} \phi$	5.4[10 ⁻³]	+5.8 -5.0	+0.1 -0.1	-0.5 +0.0	-0.2 +0.5	-0.5 +0.7	+994.6 -1005.4	+0.9 -0.8	+0.6 -0.6	+0.4 -0.6
$B^- \rightarrow \bar{K}^{*0} \rho^-$	6.0[10 ⁻³]	+5.2 -4.5	+1.3 -1.1	+0.2 -0.5	-0.1 +0.4	-0.6 +1.1	+994.0 -1006.0	+0.5 -0.5	+0.7 -0.7	+0.5 -0.7
$\bar{B}_d \rightarrow \bar{K}^{*0} \rho^0$	-3.7[10 ⁻¹]	+0.3 -0.2	-0.3 +0.3	-2.6 +1.4	+0.7 -1.6	-0.3 +0.0	+13.7 -6.3	+2.1 -1.8	-0.3 +0.3	-0.4 +0.5
$\bar{B}_d \rightarrow \bar{K}^{*0} \omega$	2.1[10 ⁻¹]	-0.1 +0.1	+0.2 -0.2	+2.0 -0.8	-0.5 +2.0	-0.1 +0.6	+7.9 -11.0	+1.5 -1.5	+0.2 -0.2	+0.1 -0.2
$B_d \rightarrow \bar{K}^{*0} \phi$	1.1[10 ⁻²]	+0.4 -0.4	+0.0 -0.0	+0.3 -0.2	-0.1 +0.3	-0.2 +0.4	+98.9 -101.1	+0.2 -0.1	+0.1 -0.1	+0.1 -0.1
$\bar{B}_d \rightarrow K^{*-} \rho^+$	3.3[10 ⁻¹]	-1.2 +1.1	-0.2 +0.2	+0.7 -0.5	-0.0 +0.1	-0.0 +0.1	+6.7 -13.2	+0.1 -0.1	+0.2 -0.3	-0.5 +0.6
$\bar{B}_s \rightarrow \rho^0 \phi$	3.0[10 ⁻¹]	+0.0 -0.0	—	+0.2 -0.2	-0.2 +0.3	-0.4 +0.8	—	+2.5 -2.8	+0.3 -0.3	+0.0 -0.1
$\bar{B}_s \rightarrow \omega \phi$	9.0[10 ⁻¹]	$A_0^{+0.8}$ -1.9	—	-7.0 +0.8	+0.9 -8.0	+0.0 -3.4	—	+1.0 -18.0	-0.5 +0.4	-0.3 +0.0
$\bar{B}_s \rightarrow \phi \phi$	9.7[10 ⁻³]	+4.0 -3.4	—	+2.4 -1.6	-0.6 +1.8	-1.5 +3.1	+30.8 -6.8	+1.5 -1.2	+1.1 -1.1	+0.7 -1.1
$\bar{B}_s \rightarrow K^{*+} K^{*-}$	2.6[10 ⁻¹]	-1.0 +0.9	-0.2 +0.1	+0.5 -0.3	-0.0 +0.1	+0.2 -0.3	+7.0 -9.0	+0.1 -0.1	+0.2 -0.2	-0.4 +0.4
$\bar{B}_s \rightarrow \bar{K}^{*0} K^{*0}$	8.7[10 ⁻³]	+3.3 -2.9	+0.9 -0.9	+1.6 -1.2	-0.3 +0.9	-1.2 +2.3	+19.7 -4.9	+0.6 -0.6	+1.0 -1.0	+0.6 -1.0

form

$$A(\bar{B} \rightarrow M_1 M_2) \sim e^{-i\gamma} - p e^{i\phi} \quad (123)$$

with p, ϕ, γ real, leads to the direct CP asymmetry

$$A_{CP} = \frac{2p \sin \phi \sin \gamma}{1 + p^2 - 2p \cos \phi \cos \gamma} \quad (124)$$

For $\sin \gamma \approx 0.92$, a value $p = \mathcal{O}(1)$ and a substantial phase ϕ give a large asymmetry. In the case of $\bar{B}_d \rightarrow \rho_L^0 \rho_L^0$ the central values $p = 0.36$, $\phi = 49^\circ$ give $A_{CP} = 53\%$.

5.3 Sensitivity to ω - ϕ mixing

In the other sections of this paper the vector mesons ϕ and ω are always implemented as pure $s\bar{s}$ and $(u\bar{u} + d\bar{d})/\sqrt{2}$ -states, respectively. Here we investigate the sensitivity of our results to the deviation from this case of ideal mixing. We assume that other effects with Zweig-rule suppression are negligibly small. We neglect, for example, Zweig-rule forbidden matrix elements of the type $\langle \phi(s\bar{s}) | (\bar{u}b)_{V-A} | B^- \rangle$.

Mixing can be introduced by the following parametrization:

$$\phi(1020) = s\bar{s} \cos \theta + \frac{u\bar{u} + d\bar{d}}{\sqrt{2}} \sin \theta \quad (125)$$

$$\omega(782) = \frac{u\bar{u} + d\bar{d}}{\sqrt{2}} \cos \theta - s\bar{s} \sin \theta. \quad (126)$$

The ideal mixing angle in this parametrization is $\theta = 0$. According to sum-rules quadratic in meson masses [28], the mixing angle can be estimated to be $\theta = 3.4^\circ$. The results of varying the mixing angle up to $\theta = 6.8^\circ$ are shown in Table 8. For most branching

Table 8: Dependence of $B \rightarrow V_L V_L$ branching fractions on ω - ϕ mixing. The variation of the branching fractions is given for two values of the mixing angle θ . The upper (lower) value corresponds to $\theta = 6.8^\circ$ ($\theta = 3.4^\circ$).

mode	default value	deviation	mode	default value	deviation
$B^- \rightarrow \rho^- \omega$	15.5[10 ⁻⁶]	$\begin{smallmatrix} -0.2 \\ -0.0 \end{smallmatrix}$	$B^- \rightarrow K^{*-} \omega$	1.7[10 ⁻⁶]	$\begin{smallmatrix} -0.4 \\ -0.2 \end{smallmatrix}$
$B^- \rightarrow \rho^- \phi$	6.0[10 ⁻⁹]	$\begin{smallmatrix} +207.5 \\ +49.8 \end{smallmatrix}$	$B^- \rightarrow K^{*-} \phi$	4.1[10 ⁻⁶]	$\begin{smallmatrix} +0.4 \\ +0.2 \end{smallmatrix}$
$\bar{B}_d \rightarrow \rho^0 \omega$	8.0[10 ⁻⁸]	$\begin{smallmatrix} +0.2 \\ +0.1 \end{smallmatrix}$	$\bar{B}_d \rightarrow \bar{K}^{*0} \omega$	1.4[10 ⁻⁶]	$\begin{smallmatrix} -0.5 \\ -0.3 \end{smallmatrix}$
$\bar{B}_d \rightarrow \omega \omega$	5.0[10 ⁻⁷]	$\begin{smallmatrix} -0.1 \\ -0.0 \end{smallmatrix}$	$\bar{B}_d \rightarrow \bar{K}^{*0} \phi$	3.7[10 ⁻⁶]	$\begin{smallmatrix} +0.5 \\ +0.3 \end{smallmatrix}$
$\bar{B}_d \rightarrow \rho^0 \phi$	2.8[10 ⁻⁹]	$\begin{smallmatrix} -1.9 \\ -1.2 \end{smallmatrix}$	$\bar{B}_s \rightarrow \rho^0 \phi$	5.9[10 ⁻⁷]	$\begin{smallmatrix} -0.1 \\ -0.0 \end{smallmatrix}$
$\bar{B}_d \rightarrow \omega \phi$	2.4[10 ⁻⁹]	$\begin{smallmatrix} +10.0 \\ +1.7 \end{smallmatrix}$	$\bar{B}_s \rightarrow \omega \phi$	4.4[10 ⁻⁸]	$\begin{smallmatrix} +28.7 \\ +4.6 \end{smallmatrix}$
$\bar{B}_s \rightarrow K^{*0} \omega$	6.5[10 ⁻⁷]	$\begin{smallmatrix} -0.6 \\ -0.3 \end{smallmatrix}$	$\bar{B}_s \rightarrow \phi \phi$	15.5[10 ⁻⁶]	$\begin{smallmatrix} -0.3 \\ -0.0 \end{smallmatrix}$
$\bar{B}_s \rightarrow K^{*0} \phi$	3.4[10 ⁻⁷]	$\begin{smallmatrix} +0.6 \\ +0.3 \end{smallmatrix}$	$\bar{B}_s \rightarrow \omega \omega$	3.2[10 ⁻⁸]	$\begin{smallmatrix} +1.6 \\ +0.3 \end{smallmatrix}$
$\bar{B}_d \rightarrow \phi \phi$	2.5[10 ⁻⁹]	$\begin{smallmatrix} -0.4 \\ -0.3 \end{smallmatrix}$	$\bar{B}_s \rightarrow \rho^0 \omega$	1.5[10 ⁻⁹]	$\begin{smallmatrix} +11.1 \\ +3.5 \end{smallmatrix}$

fractions the effect of a nonvanishing mixing angle $\theta \approx 3.4^\circ$ is very small, in particular for the important modes $B^- \rightarrow \rho^- \omega$, $B^- \rightarrow K^{*-} \phi$, $\bar{B}_s \rightarrow \phi \phi$. On the other hand, the modes $\bar{B}_d \rightarrow \rho^0 \phi$, $\bar{B}_d \rightarrow \omega \phi$, $\bar{B}_s \rightarrow \omega \phi$, $\bar{B}_s \rightarrow \rho^0 \omega$ have a significant dependence on deviations from ideal mixing. The largest effect is observed for $B^- \rightarrow \rho^- \phi$. In this case $B^- \rightarrow \rho^- \omega$ feeds into the former channel through mixing with a more than three orders of magnitude higher branching ratio compared to $B^- \rightarrow \rho^- \phi(s\bar{s})$, which overcompensates the small mixing angle:

$$B(B^- \rightarrow \rho^- \phi)_{\text{mix}} \approx \sin^2 \theta B(B^- \rightarrow \rho^- \omega) \quad (127)$$

A recent discussion of hadronic B decays, mostly with charm in the final state, for which ω - ϕ mixing has a large impact can be found in [35]. Their estimate of $B^- \rightarrow \rho^- \phi$ is compatible with ours.

5.4 Unitarity triangle from CP violation in $B_d \rightarrow \rho_L^+ \rho_L^-$

5.4.1 Determination of $\bar{\rho}$, $\bar{\eta}$, γ and α

The time dependent CP asymmetry in $B_d \rightarrow \rho_L^+ \rho_L^-$ is given by

$$\mathcal{A}_{CP,\rho}(t) = \frac{\Gamma(\bar{B}_d(t) \rightarrow \rho_L^+ \rho_L^-) - \Gamma(B_d(t) \rightarrow \rho_L^+ \rho_L^-)}{\Gamma(\bar{B}_d(t) \rightarrow \rho_L^+ \rho_L^-) + \Gamma(B_d(t) \rightarrow \rho_L^+ \rho_L^-)} = S_\rho \sin(\Delta m_d t) - C_\rho \cos(\Delta m_d t) \quad (128)$$

The parameters S_ρ and C_ρ have been measured to be

$$S_\rho = -0.05 \pm 0.17 \quad C_\rho = -0.06 \pm 0.13 \quad (129)$$

as quoted by [24], based on results of BaBar [36] and Belle [37]. Together with the experimentally well determined quantity $\sin 2\beta$ from CP violation in $B \rightarrow \psi K^0$ decays, the parameter S_ρ can be used to fix the CKM unitarity triangle. The value of $\sin 2\beta$ from Table 3 implies $\beta = (21.5 \pm 1.0)^\circ$ or

$$\tau \equiv \cot \beta = 2.54 \pm 0.13 \quad (130)$$

In terms of the improved Wolfenstein parameters $\bar{\rho}$ and $\bar{\eta}$ [38] the unitarity triangle is then determined by

$$\bar{\rho} = 1 - \tau \bar{\eta} \quad (131)$$

$$\bar{\eta} = \frac{1}{(1 + \tau^2)S_\rho} \left[(1 + \tau S_\rho)(1 + r_\rho \cos \phi_\rho) - \sqrt{(1 - S_\rho^2)(1 + r_\rho \cos \phi_\rho)^2 - S_\rho(1 + \tau^2)(S_\rho + \sin 2\beta)r_\rho^2 \sin^2 \phi_\rho} \right] \quad (132)$$

These formulas have been derived in [19,20] for $B \rightarrow \pi^+ \pi^-$, but they apply to the case of $B \rightarrow \rho_L^+ \rho_L^-$ as well. The parameters r_ρ and ϕ_ρ are hadronic quantities. They are defined here through

$$r_\rho e^{i\phi_\rho} = -\frac{a_4^c + a_{10}^c + r_A^\rho (b_3 + 2b_4 - \frac{1}{2}b_3^{\text{EW}} + \frac{1}{2}b_4^{\text{EW}})}{a_1 + a_4^u + a_{10}^u + r_A^\rho (b_1 + b_3 + 2b_4 - \frac{1}{2}b_3^{\text{EW}} + \frac{1}{2}b_4^{\text{EW}})} \quad (133)$$

where all coefficients a_i , b_i refer to the $\rho_L^+ \rho_L^-$ final state and

$$r_A^\rho \equiv \frac{B_{\rho\rho}}{A_{\rho\rho}} = \frac{f_B f_\rho}{m_B^2 A_0^{B \rightarrow \rho}(0)} \approx 5 \cdot 10^{-3} \quad (134)$$

The real quantities r_ρ and ϕ_ρ are the magnitude and phase of the penguin-to-tree amplitude ratio in $\bar{B} \rightarrow \rho_L^+ \rho_L^-$. They are independent of CKM parameters. Numerically we

find

$$r_\rho = 0.038 \pm 0.005 (\mu, \alpha_2^\rho) \quad {}^{+0.019}_{-0.026} (\rho_A, \phi_A) \quad (135)$$

$$\phi_\rho = 0.23 \pm 0.09 (m_c, \alpha_2^\rho) \quad {}^{+0.74}_{-0.73} (\rho_A, \phi_A) \quad (136)$$

$$r_\rho \cos \phi_\rho = 0.037 \pm 0.005 (\mu, \alpha_2^\rho) \quad {}^{+0.018}_{-0.026} (\rho_A, \phi_A) \quad (137)$$

The first error is from the uncertainties in the input parameters A_0 , α_2^ρ , f_ρ^\perp , λ_B , f_B , m_c and a variation of the renormalization scale μ between $m_b/2$ and $2m_b$ around its default value $\mu = m_b$. The dominant sources of uncertainty are indicated in brackets. The second error reflects the sensitivity to the parameters ρ_A , ϕ_A , ρ_H and ϕ_H used to model power corrections from weak annihilation (A) and in the spectator scattering amplitude (H). We have used $0 \leq \rho_{A,H} \leq 1$, $0 \leq \phi_{A,H} \leq 2\pi$. The second error is entirely determined by weak annihilation.

The phase ϕ_ρ is parametrically suppressed since it arises only at order α_s or Λ_{QCD}/m_b . Its precise value is rather uncertain, in particular due to the model dependence of power corrections, which may compete numerically with the calculable $\mathcal{O}(\alpha_s)$ term. Fortunately the dependence of $\bar{\eta}$ in (132) on ϕ_ρ is very weak [19,20]. In addition, r_ρ is a small parameter, even smaller than the corresponding quantity r_π in $\bar{B}_d \rightarrow \pi^+\pi^-$. The smaller size of the penguin contribution in the case of vector mesons as compared to pseudoscalars has been pointed out before in the context of QCD factorization [9,23]. The formulation in (132) makes it particularly transparent to analyze the impact of a small penguin correction on the determination of the unitarity triangle. To linear order in r_ρ , eq. (132) implies the simple relation

$$\bar{\eta} = \frac{1 + \tau S_\rho - \sqrt{1 - S_\rho^2}}{(1 + \tau^2) S_\rho} (1 + r_\rho \cos \phi_\rho) \quad (138)$$

In this approximation $\bar{\eta}$ and $\bar{\rho}$ depend only on the real part of the penguin-to-tree ratio. As can be seen from (132), second order corrections in r_ρ are further suppressed by $\sin^2 \phi_\rho$.

With $\bar{\eta}$ and $\bar{\rho}$ also the CKM angles γ and α can be computed:

$$\gamma = \arctan \frac{\bar{\eta}}{1 - \tau \bar{\eta}}, \quad \alpha = \pi - \beta - \gamma \quad (139)$$

It is instructive to write down the expressions for small values of S_ρ , which are suggested by the data in (129). To first order in both S_ρ and r_ρ we find

$$\gamma = \arctan \tau + \frac{S_\rho}{2} + \tau r_\rho \cos \phi_\rho \quad (140)$$

$$\alpha = \frac{\pi}{2} - \frac{S_\rho}{2} - \tau r_\rho \cos \phi_\rho \quad (141)$$

For $S_\rho = 0$ and in the absence of a penguin contribution one has $\alpha = 90^\circ$ and $\gamma = (68.5 \pm 1.0)^\circ$. Non-zero values of the observable S_ρ and the theoretical quantity $r_\rho \cos \phi_\rho$ then compete in shifting γ and α away from these lowest-order approximations.

Evaluation of the exact formulas (132) and (139) gives

$$\bar{\eta} = 0.350 \pm 0.013(\tau) \pm 0.012(S_\rho) \pm 0.008(r_\rho \cos \phi_\rho) \quad (142)$$

$$\gamma = 72.4^\circ \pm 1.3^\circ(\tau) \pm 5.1^\circ(S_\rho) \pm 3.2^\circ(r_\rho \cos \phi_\rho) \quad (143)$$

Nearly identical results are obtained for γ when the first order expression (140) is employed. The approximations (140) and (141) work to very good accuracy in the relevant range of S_ρ and r_ρ . This greatly facilitates the determination of γ and α and the analysis of errors, which can simply be read off from (140) and (141).

The calculation of γ in [11] using the longitudinal part of the time dependent CP-asymmetry in the $\rho^+\rho^-$ -system and β as input yields a similar result for the hadronic error of $\pm 3^\circ$.

The determination of γ in (143) is considerably more precise at present than measurements using $B \rightarrow DK$ tree-level decays. Belle has found [39]

$$\gamma = (53_{-18}^{+15}(\text{stat}) \pm 3(\text{sys}) \pm 9(\text{model}))^\circ \quad (144)$$

and a recent analysis from BaBar gives [40]

$$\gamma = (76 \pm 22(\text{stat}) \pm 5(\text{sys}) \pm 5(\text{model}))^\circ \quad (145)$$

Within the errors both are well compatible with (143).

5.4.2 Bounds on UT parameters

Useful information on the angle γ can also be obtained in the form of a lower bound, which is even less sensitive to theory input than the result in (143). It relies only on the conservative condition that $r \cos \phi \geq 0$, which holds in the heavy-quark limit. This bound has been derived in [19,20]. Further discussions may also be found in [41,42]. The bound is valid as long as $S > -\sin 2\beta$ and reads

$$\gamma > \frac{\pi}{2} - \arctan \frac{S - \tau(1 - \sqrt{1 - S^2})}{\tau S + 1 - \sqrt{1 - S^2}} \quad (146)$$

The constraint (146) can be evaluated using CP violation in $B \rightarrow \pi^+\pi^-$ ($S = S_\pi$) or in $B \rightarrow \rho_L^+\rho_L^-$ ($S = S_\rho$). The derivation of (146) is identical for both cases. In fact, since the (positive) penguin correction $r_\rho \cos \phi_\rho$ is smaller than $r_\pi \cos \phi_\pi$, the bound is expected to be more stringent using S_ρ instead of S_π . This expectation is indeed borne out by the experimental result $S_\rho > S_\pi = -0.61 \pm 0.08$ (see sec. 5.7), which implies that S_ρ gives the better constraint. Qualitatively, these features can also be understood from the approximate relation (140).

To linear order in S the bound (146) becomes

$$\gamma > \arctan \tau + \frac{S}{2} \quad (147)$$

in agreement with (140).

Using $S = S_\rho = -0.05$ (central), -0.22 (1σ), -0.39 (2σ), we obtain from (146), respectively

$$\gamma > 67^\circ, \quad 62^\circ, \quad 57^\circ \quad (148)$$

The linear approximation (147) gives practically identical results. We remark that the relevant values of S_ρ fulfill the condition $S_\rho > -\sin 2\beta$, under which the bound can be applied.

The penguin correction is expected to shift the numbers in (148) by approximately $+6^\circ$ to yield the actual value of γ . The bound is therefore quite stringent. Within a Standard Model interpretation it eliminates already a sizable fraction of the allowed range from the direct measurements in (144) and (145).

Bounds similar to the one for γ can also be derived for $\bar{\eta}$ and $\bar{\rho}$ [19,20]. The lower bound for $\bar{\eta}$ is given by the right-hand side of (138) with r_ρ put to zero, the upper bound on $\bar{\rho}$ then follows from $\bar{\rho} = 1 - \tau\bar{\eta}$. With the same input for S_ρ as in (148) we find

$$\bar{\eta} > 0.338, \quad 0.326, \quad 0.314 \quad (149)$$

and

$$\bar{\rho} < 0.143, \quad 0.172, \quad 0.203 \quad (150)$$

5.4.3 Precision determination of $|V_{ub}|$ from $\sin 2\beta$ and S_ρ

The preceding analysis has a further interesting application regarding the determination of $|V_{ub}|$ from $\sin 2\beta$ and S_ρ . The value of $|V_{ub}|$ determined in this way may be affected by New Physics entering CP violation in $B_d \rightarrow \psi K_S$ and $B_d \rightarrow \rho_L^+ \rho_L^-$. The presence of non-standard contributions can be revealed by comparing the extracted value of $|V_{ub}|$ with the result for $|V_{ub}|$ from an independent method. An important example is the direct determination of $|V_{ub}|$ from semileptonic, exclusive or inclusive, $b \rightarrow ul\nu$ decays, which are most likely independent of physics beyond the Standard Model. It is clear that the usefulness of such a New Physics test will depend on how precisely $|V_{ub}|$ can be determined. We will show that $\sin 2\beta$ and S_ρ offer a particularly clean and accurate determination of $|V_{ub}|$.

The magnitude of $|V_{ub}|$ is proportional to $R_b \equiv \sqrt{\bar{\rho}^2 + \bar{\eta}^2}$. Using the exact formulas in (131) and (132), we expand R_b^2 in S_ρ and r_ρ . This is motivated by the smallness of the theoretical parameter r_ρ and the empirical observation that also S_ρ is small, as we have discussed in section 5.4.1. Treating S_ρ and r_ρ as small quantities of the same order we find

$$R_b = \sqrt{\bar{\rho}^2 + \bar{\eta}^2} = \frac{1}{\sqrt{1 + \tau^2}} \cdot \left[1 + \frac{1}{2} \left(\frac{S_\rho}{2} + \tau r_\rho \cos \phi_\rho \right)^2 + \frac{r_\rho}{2} \left(\frac{S_\rho}{2} + \tau r_\rho \cos \phi_\rho \right) (S_\rho \cos \phi_\rho + 2\tau r_\rho \sin^2 \phi_\rho) \right] \quad (151)$$

where we have neglected terms of the fourth order. Through terms of third order in S_ρ and r_ρ ($S_\rho^3, S_\rho^2 r_\rho, S_\rho r_\rho^2, r_\rho^3$) eq. (151) is exact.

The basic features of (151) are easy to understand from the geometry of the unitarity triangle. If $S_\rho = r_\rho = 0$ then $\alpha = \pi/2$. In this case $R_b = \sin \beta \equiv 1/\sqrt{1 + \tau^2}$, which gives the leading term in (151). Because $\sin \beta$ is the minimum value that R_b can take for fixed β , first order corrections in r_ρ and S_ρ are absent and the second-order term is strictly positive. The protection of (151) from first-order corrections in S_ρ and r_ρ is the basis for a precise determination of V_{ub} .

The quantity $S_\rho/2 + \tau r_\rho \cos \phi_\rho$ appeared already in (140), (141). For $S_\rho < 0$ there is a further cancellation in this term with the penguin shift $\tau r_\rho \cos \phi_\rho$. Taking $S_\rho = -0.05 \pm 0.17$ (129), $\tau = 2.54 \pm 0.13$ (130) and the conservative range $r_\rho \cos \phi_\rho = 0.04 \pm 0.03$ we have

$$\frac{S_\rho}{2} + \tau r_\rho \cos \phi_\rho = 0.077 \pm 0.114 \quad (152)$$

The range of $r_\rho \cos \phi_\rho$ covers the result obtained from the QCD analysis in sec. 5.4.1. As we will show in sec. 5.6, $r_\rho \cos \phi_\rho$ can also be determined by independent experimental information on the penguin mode $\bar{B}_d \rightarrow \bar{K}_L^{*0} K_L^{*0}$, which confirms the values employed here.

Through second order in S_ρ and r_ρ the correction factor relative to the lowest-order result in (151) reads, using (152),

$$1 + \frac{1}{2} \left(\frac{S_\rho}{2} + \tau r_\rho \cos \phi_\rho \right)^2 = 1.003_{-0.003}^{+0.015} \quad (153)$$

We remark that the lower limit of 1 for this factor is an absolute bound. The third-order term in (151) is less than about $0.2 r_\rho S_\rho / 2 \lesssim 0.2 \cdot 0.04 \cdot 0.1 \lesssim 0.001$ and thus completely negligible.

Using $\sin \beta = 0.366 \pm 0.016$ from Table 3 we obtain

$$R_b = \sin \beta \left[1 + \frac{1}{2} \left(\frac{S_\rho}{2} + \tau r_\rho \cos \phi_\rho \right)^2 \right] = 0.367 \pm 0.016_{-0.002}^{+0.005} \quad (154)$$

From [28] we have

$$\lambda = |V_{us}| = 0.226 \pm 0.002 \quad |V_{cb}| = 0.0416 \pm 0.0006 \quad (155)$$

This implies

$$|V_{ub}| \equiv \left| \frac{V_{cb} V_{cd}}{V_{ud}} \right| R_b = \frac{\lambda}{1 - \frac{\lambda^2}{2}} R_b |V_{cb}| = (3.54_{-0.15}^{+0.16}(R_b) \pm 0.05(V_{cb}) \pm 0.03(V_{us})) \cdot 10^{-3} \quad (156)$$

The uncertainty is dominated by the error in β ($(\pm 0.15) \cdot 10^{-3}$), followed by the error in the correction from S_ρ, r_ρ ($(\pm 0.05) \cdot 10^{-3}$) and the error in V_{cb} . Adding errors in quadrature the final result reads

$$|V_{ub}| = (3.54 \pm 0.17) \cdot 10^{-3} \quad (157)$$

It corresponds to a ratio $|V_{ub}/V_{cb}| = 0.085 \pm 0.004$, in agreement with Table 3. The value in (157) should be compared with the direct measurements of $|V_{ub}|$ in $b \rightarrow ul\nu$ transitions. A recent analysis of inclusive decays gives [43]

$$|V_{ub}| = (3.70 \pm 0.32) \cdot 10^{-3} \quad (158)$$

The exclusive determination from $B \rightarrow \pi l\nu$ decays has been investigated in [44] with the result

$$|V_{ub}| = (3.36 \pm 0.23) \cdot 10^{-3} \quad (159)$$

Related discussions, in the context of QCD sum rules, can be found for instance in [45] and [46]. Using an average of data from lattice QCD, [47] quotes for the determination from exclusive decays

$$|V_{ub}| = (3.54 \pm 0.40) \cdot 10^{-3} \quad (160)$$

The results in (157), (158), (159) and (160) are in very good agreement with each other. They provide us with a test of Standard Model CP violation in $B \rightarrow \psi K_S$ and $B \rightarrow \rho^+ \rho^-$ (157) against the $|V_{ub}|$ determination from tree-level, semileptonic $b \rightarrow ul\nu$ decays (158), (159) and (160).

Numbers for $|V_{ub}|$ very similar to (157) have been obtained from global fits of the unitarity triangle performed by the CKMfitter [29] and UTfit [30] collaborations, which quote

$$|V_{ub}| = (3.57 \pm 0.17) \cdot 10^{-3} \quad (\text{CKMfitter}) \quad (161)$$

$$|V_{ub}| = (3.55 \pm 0.15) \cdot 10^{-3} \quad (\text{UTfit}) \quad (162)$$

While such global fit results summarize our current overall knowledge of quark-mixing parameters, they do not exhibit explicitly the individual pieces of information that determine this knowledge. We emphasize here that the precise result in (157) can be obtained from $\sin 2\beta$ and S_ρ alone, with only very moderate requirements on the accuracy of the penguin contribution $\sim r_\rho$ from theory. The representation proposed in (154) makes this statement particularly transparent.

The result in (157) is currently the most precise determination of $|V_{ub}|$. Since the error is dominated by the uncertainty in $\sin \beta$, an even higher precision will be achieved by a more accurate measurement of $\sin \beta$ as it is expected at the upcoming LHC experiments. For instance, with a determination of $\sin \beta$ to 1%, the error in (157) would shrink to $\pm 0.08 \cdot 10^{-3}$, corresponding to a precision of 2% for $|V_{ub}|$.

Constraint on New Physics phase in $B_d - \bar{B}_d$ mixing

The preceding analyses rely on the assumption of a Standard Model phase in $B_d - \bar{B}_d$ mixing. We would like to examine the effect of a small New Physics phase entering only in $B_d - \bar{B}_d$ -meson mixing [48,49]. In this scenario the New Physics phase shall not violate unitarity of the Standard Model CKM matrix. The modified mixing phase $\beta + \Omega$, with the New Physics contribution Ω , enters the analysis in the determination

of $\tau = \cot(\beta + \Omega)$ from $\bar{B}_d \rightarrow J/\psi K_s$ and through mixing-induced CP violation in $\bar{B}_d \rightarrow \rho^+ \rho^-$. The relation (131) for $\bar{\rho}$ will depend now on Ω :

$$\bar{\rho} = \frac{(1 - \tau \bar{\eta}) - (\tau + \bar{\eta}) \tan \Omega}{1 - \tau \tan \Omega} \quad (163)$$

The measurement of S_ρ determines $\bar{\eta}$ up to the mixing phase Ω . The new relation for $\bar{\eta}$ in an expansion in r_ρ and S_ρ reads

$$\bar{\eta} = \frac{\tau(1 - \tau \tan \Omega)}{1 + \tau^2} + \frac{(1 - \tau \tan \Omega) \left(\tau r_\rho \cos \phi_\rho + \frac{S_\rho}{2} (1 - \tau \tan \Omega) \right)}{1 + \tau^2} + \mathcal{O}(r_\rho^2, r_\rho S_\rho, S_\rho^2) \quad (164)$$

We note that Ω enters the leading term in the expansion with an enhancement of $\tau \approx 2.5$. The first order term is suppressed relative to the leading order term by a factor of ~ 0.1 .

Using the exact relations for $\bar{\rho}$ and $\bar{\eta}$ one finds the following expansion for R_b :

$$R_b = \frac{|1 - \tau \tan \Omega|}{\sqrt{1 + \tau^2}} \left[1 - \tan \Omega \left(\frac{\tau r_\rho \cos \phi_\rho}{1 - \tau \tan \Omega} + \frac{S_\rho}{2} \right) \right] + \mathcal{O}(r_\rho^2, r_\rho S_\rho, S_\rho^2) \quad (165)$$

Again we have an enhancement of the dependence on Ω by τ . For R_b the error from S_ρ and $r_\rho \cos \phi_\rho$ is much less important than the error from τ (130), in contrast to the case of $\bar{\eta}$ (142).

Relating R_b to $|V_{ub}|$ as in (156), taking $|V_{ub}|$, S_ρ , τ from experiment and r_ρ and ϕ_ρ from QCD factorization, the angle Ω can be extracted. In general the solution is not unique. Here we assume that the new phase Ω is small, neglecting discrete ambiguities. Such ambiguities may be eliminated with additional measurements. In particular, a second solution with large Ω would imply a negative sign of $\cos(2(\beta + \Omega))$, which is disfavoured by experiment [50]. A more general discussion on the New Physics aspects of this analysis can be found in [49].

If one disregards solutions with $|\Omega| > \arctan(1/\tau) \approx 20^\circ$ and uses the exclusive determination (160) of $|V_{ub}|$, then Ω can be determined with an accuracy of few degrees. Using the exact expression for $R_b(\tau, S_\rho, r_\rho, \phi_\rho, \Omega)$ we find

$$\Omega = (0.0_{+1.0}^{-0.9}(\tau)_{-0.1}^{+0.2}(S_\rho)_{-0.1}^{+0.2}(r_\rho)_{-0.3}^{+0.3}(V_{cb})_{+2.5}^{-2.5}(V_{ub}))^\circ \quad (166)$$

One may note the very small impact of $S_\rho = -0.05 \pm 0.17$ and $r_\rho = 0.04 \pm 0.03$. A different value for $|V_{ub}|$ from other direct determinations such as (158) or (159) leads to very similar results. Combining the errors in (166) in quadrature one finds $\Omega = (0.0 \pm 2.7)^\circ$.

5.5 Extracting r_ρ from $B^- \rightarrow \bar{K}_L^{*0} \rho_L^-$

The precision of CKM angles extracted from CP violation in $B \rightarrow \rho_L^+ \rho_L^-$ is ultimately limited by our knowledge of the penguin parameters r_ρ and, to a lesser extent, ϕ_ρ . Since r_ρ is small, a very moderate accuracy in this quantity is sufficient to obtain a small theoretical error for CKM parameters. In [51] it has been proposed to constrain the

penguin parameter r_ρ using the penguin dominated decay $B^- \rightarrow \bar{K}_L^{*0} \rho_L^-$. We will discuss this method in the context of our analysis, comment on the benefits and limitations, present an updated numerical evaluation, and compare with the theory results of sec. 5.4.

The main idea of [51] is to determine the penguin amplitude from the pure-penguin process $B^- \rightarrow \bar{K}_L^{*0} \rho_L^-$ through

$$B(B^- \rightarrow \bar{K}_L^{*0} \rho_L^-) = \frac{\tau_{B_u} G_F^2 |\lambda'_c|^2}{32\pi m_B} |a_c(\rho K^*)|^2 \quad (167)$$

Here we defined $a_p(\rho K^*) \equiv a_p(B^- \rightarrow \bar{K}_L^{*0} \rho_L^-)$ as the coefficient of $(iG_F/\sqrt{2})\lambda_p$ in the amplitude for $B^- \rightarrow \bar{K}_L^{*0} \rho_L^-$, eqs. (67) and (106). They correspond to the charm- and up-quark penguin amplitudes for this process. Since $a_u(\rho K^*)$ and $a_c(\rho K^*)$ are of comparable size, and the up-quark amplitude is strongly CKM suppressed, the charm penguin completely dominates the branching ratio (167). The penguin amplitude $a_c(\rho K^*)$ can be related to the (similarly normalized) penguin amplitude $a_c(\rho)$ in $\bar{B}_d \rightarrow \rho^+ \rho^-$ by introducing the factor

$$|\kappa| = \left| \frac{a_c(\rho K^*)}{a_c(\rho)} \right| \approx 0.84 \quad (168)$$

To lowest order (in α_s and Λ/m_b) this factor would be given by $\kappa = f_K^*/f_\rho = 1.04$. Including QCD corrections this value is reduced to $|\kappa| = 1.01$, and further to $|\kappa| = 0.97$ by the effects of electroweak penguins. The estimate in (168) includes also the weak annihilation terms with default model parameters. Annihilation contributions are thus seen to be potentially important. These observations agree with the discussion in [51]. In that paper the ratio of the penguin amplitudes in $B^- \rightarrow \bar{K}_L^{*0} \rho_L^-$ and $\bar{B}_d \rightarrow \rho^+ \rho^-$ has been parametrized in terms of a factor F , which is related to κ through $|\kappa| = \sqrt{F} f_{K^*}/f_\rho$. In [51] a rather wide range for F is assumed, $0.3 < F < 1.5$. We will use the same range, which corresponds to $|\kappa| = 0.93 \pm 0.36$.

For a given value of $|\kappa|$ the penguin parameters r_ρ , ϕ_ρ are then constrained by the ratio

$$\frac{B(B^- \rightarrow \bar{K}_L^{*0} \rho_L^-)}{B(\bar{B} \rightarrow \rho_L^+ \rho_L^-)} = \frac{\tau_{B_u}}{\tau_{B_d}} \left| \frac{V_{cs}}{V_{cd}} \right|^2 \frac{|\kappa|^2 r_\rho^2}{\bar{\rho}^2 + \bar{\eta}^2 + r_\rho^2 + 2\bar{\rho} r_\rho \cos \phi_\rho} \quad (169)$$

where CP averaged rates are understood. Using $\tau = \cot \beta$, S_ρ , C_ρ and the ratio of branching fractions in (169) as experimental inputs, the four quantities $\bar{\rho}$, $\bar{\eta}$, r_ρ and ϕ_ρ can be determined as functions of $|\kappa|$. A discrete ambiguity in the sign of $\cos \phi_\rho$ can be resolved using the heavy-quark limit. The suppression of ϕ_ρ in this limit singles out the solution with $\cos \phi_\rho > 0$. A similar use of the qualitative result $\cos \phi_\rho > 0$ from factorization has been made in [19,20]. Further details on the extraction of $\bar{\rho}$, $\bar{\eta}$, r_ρ , ϕ_ρ are discussed in 5.6 in the context of a similar analysis. The results for the present method are collected in Table 9. Combining and symmetrizing errors we obtain from Table 9

$$\gamma = (72.5 \pm 6.9)^\circ \quad \alpha = \pi - \beta - \gamma = (86.0 \pm 7.0)^\circ \quad (170)$$

Table 9: CKM and penguin parameters extracted from $\tau = \cot \beta = 2.54 \pm 0.13$, $S_\rho = -0.05 \pm 0.17$, $C_\rho = -0.06 \pm 0.13$ and $b = B(B^- \rightarrow \bar{K}_L^{*0} \rho_L^-) / B(\bar{B}^- \rightarrow \rho_L^+ \rho_L^-) = 0.186 \pm 0.049$. The penguin correction factor is taken to be $|\kappa| = 0.93 \pm 0.36$.

	central	τ	S_ρ	C_ρ	b	$ \kappa $
$\bar{\rho}$	0.110	-0.010 $+0.012$	-0.030 $+0.031$	-0.002 $+0.028$	-0.005 $+0.005$	$+0.010$ -0.024
$\bar{\eta}$	0.350	-0.013 $+0.014$	$+0.012$ -0.012	$+0.001$ -0.011	$+0.002$ -0.002	-0.004 $+0.009$
$\gamma[\text{deg}]$	72.5	$+1.0$ -1.1	$+5.0$ -5.1	$+0.3$ -4.8	$+0.8$ -0.9	-1.7 $+3.9$
r_ρ	0.040	-0.002 $+0.002$	$+0.000$ -0.000	$+0.000$ -0.001	$+0.005$ -0.006	-0.011 $+0.027$
ϕ_ρ	-0.32	$+0.00$ -0.00	$+0.01$ -0.01	$+0.69$ -1.17	$+0.04$ -0.06	-0.13 $+0.13$

where S_ρ is the largest source of uncertainty. The results agree very well with those in (143). Eq. (170) is an update of the results quoted in [51]. We have checked that we obtain the numbers given in that paper if we use the same input.

A disadvantage of the method just described is that the charm-penguin amplitudes in $B^- \rightarrow \bar{K}_L^{*0} \rho_L^-$ and in $\bar{B}_d \rightarrow \rho_L^+ \rho_L^-$ are not related in full QCD by $SU(3)$ flavour symmetry alone. The $SU(3)$ argument relating $a_c(\rho K^*)$ and $a_c(\rho)$ strictly holds only to leading order in the heavy-quark limit. At the level of power corrections from weak annihilation these penguin amplitudes are not related by $SU(3)$. This can be seen from eqs. (95) and (106), which show that the QCD annihilation penguins are determined by the coefficient b_3 for $a_c(\rho K^*)$, but by $b_3 + 2b_4$ instead for $a_c(\rho)$. This difference has been discussed in [51]. In order to account for the corresponding $SU(3)$ breaking, a rather generous correction factor κ (168) has been allowed for. While this is certainly a valid procedure, it is somewhat against the spirit of using experimental data to constrain the penguin in $\bar{B}_d \rightarrow \rho_L^+ \rho_L^-$. An unexpectedly large penguin annihilation effect in this channel, beyond the available model estimates, would not necessarily be indicated by the $B^- \rightarrow \bar{K}_L^{*0} \rho_L^-$ rate, not even in the $SU(3)$ limit. In this respect, the method of [51] amounts to the standard analysis of CP violation in $\bar{B}_d \rightarrow \rho_L^+ \rho_L^-$ with input on r_ρ from factorization calculations, which are validated by comparing similar theory results on the penguin mode $B^- \rightarrow \bar{K}_L^{*0} \rho_L^-$ with data. Indeed, QCD factorization works very well for $B^- \rightarrow \bar{K}_L^{*0} \rho_L^-$ with little room for sizable power corrections. Correspondingly, the values for r_ρ and the angle γ determined in Table 9 are very close to the values found in the factorization analysis, eqs. (135) and (143). Nevertheless, an independent control of penguin annihilation corrections in $\bar{B}_d \rightarrow \rho_L^+ \rho_L^-$, which is not guaranteed by $B^- \rightarrow \bar{K}_L^{*0} \rho_L^-$, would be very desirable. A variant of the method in [51] that can provide this control will be discussed in the following section.

5.6 Extracting r_ρ from $B_d \rightarrow \bar{K}_L^{*0} K_L^{*0}$

In this section we propose a method to constrain the penguin parameter r_ρ in $\bar{B}_d \rightarrow \rho_L^+ \rho_L^-$ (133) using $SU(3)$ flavour symmetry and data on the penguin decay $\bar{B}_d \rightarrow \bar{K}_L^{*0} K_L^{*0}$. This approach shares the basic idea with the method discussed in section 5.5. An important difference is that now, unlike the case of section 5.5, the penguin process exhibits an exact $SU(3)$ relation to the penguin amplitude of $\bar{B}_d \rightarrow \rho_L^+ \rho_L^-$. Because this relation extends beyond the heavy-quark limit, the method offers an independent control of all power corrections, in particular those from weak annihilation topologies. We show that a precise determination of the unitarity triangle is possible, already with present data on $\bar{B}_d \rightarrow \bar{K}_L^{*0} K_L^{*0}$. Since the penguin decay $\bar{B}_d \rightarrow \bar{K}_L^{*0} K_L^{*0}$ is a $\Delta S = 0$ transition, the up-quark sector of the amplitude does not have the same CKM suppression as for the $\Delta S = 1$ process $B^- \rightarrow \bar{K}_L^{*0} \rho_L^-$. We will find that it is still sufficiently well constrained.

The $SU(3)$ relation between the relevant penguin amplitudes can be demonstrated as follows. The penguin contribution for $\bar{B}_d \rightarrow \rho_L^+ \rho_L^-$ is given by the component of the amplitude proportional to $\lambda_c = V_{cb} V_{cd}^*$. The corresponding part of the effective Hamiltonian (1) has the form

$$\mathcal{H}_{\text{QCDP},c} = \frac{G_F}{\sqrt{2}} \left(C_1 Q_1^c + C_2 Q_2^c + \sum_{i=3,\dots,6} C_i Q_i + C_{8g} Q_{8g} \right) + \text{h.c.} \quad (171)$$

where we have neglected higher-order electroweak effects. The operators Q_i are defined in (2). The Hamiltonian in (171) gives rise to the QCD penguin amplitude in the charm sector of both $\bar{B}_d \rightarrow \rho_L^+ \rho_L^-$ and $\bar{B}_d \rightarrow \bar{K}_L^{*0} K_L^{*0}$. To prove the symmetry relation we note that all operators entering (171) are invariant under $SU(2)$ rotations of the doublet (u, s) of quark flavours, the V-spin subgroup of flavour $SU(3)$. The initial state, a \bar{B}_d meson in both cases, is likewise a V-spin singlet. The final states $\rho^+ \rho^-$ and $\bar{K}^{*0} K^{*0}$ are transformed into each other by interchanging u and s quarks, which represents a particular V-spin rotation. In the V-spin symmetry limit, therefore, the relation

$$\langle \bar{K}_L^{*0} K_L^{*0} | \mathcal{H}_{\text{QCDP},c} | \bar{B}_d \rangle = \langle \rho_L^+ \rho_L^- | \mathcal{H}_{\text{QCDP},c} | \bar{B}_d \rangle \quad (172)$$

holds as an identity in QCD. As a consequence, the QCD penguin amplitudes proportional to λ_c in $\bar{B}_d \rightarrow \rho_L^+ \rho_L^-$ and $\bar{B}_d \rightarrow \bar{K}_L^{*0} K_L^{*0}$ have the same form, including the weak annihilation contributions. This can be seen from (58), (59) and (95), (96).

In practice V-spin is broken because the masses of up and strange quarks are not the same. This source of V-spin breaking can be expected to be of the typical size of flavour $SU(3)$ breaking effects, roughly 20-30%. It is possible to estimate the required correction to the V-spin limit using factorization. We will give a more quantitative treatment below. Electroweak effects also violate V-spin symmetry. They are similar to isospin breaking and likely to be much smaller than the $SU(3)$ -breaking effects due to the strange-quark mass. For example, the relative importance of (standard) electroweak penguins is governed by the ratio $a_{10}^c/a_4^c \approx 0.03$. This is safely negligible in comparison with the dominant V-spin breaking effects. Contributions from electroweak penguin annihilation are very small and can also be neglected.

We next turn to the phenomenological implications of the flavour symmetry relation (172). Denoting by $a_p(K^*) \equiv a_p(\bar{B}_d \rightarrow \bar{K}_L^{*0} K_L^{*0})$ the coefficient of $(iG_F/\sqrt{2})\lambda_p$ in the amplitude for $\bar{B}_d \rightarrow \bar{K}_L^{*0} K_L^{*0}$, eqs. (59) and (96), the CP averaged branching fraction may be written as

$$B(\bar{B}_d \rightarrow \bar{K}_L^{*0} K_L^{*0}) = \frac{\tau_{B_d} G_F^2 |\lambda_c|^2}{32\pi m_B} \left[f_0 |a_c(K^*)|^2 + 2f_1 \operatorname{Re} a_c^*(K^*) \Delta(K^*) + f_2 |\Delta(K^*)|^2 \right] \quad (173)$$

$$\Delta(K^*) = a_c(K^*) - a_u(K^*) \quad (174)$$

where the functions f_i depend only on CKM parameters. Expressed in terms of $\tau = \cot \beta$ from (130) and

$$\sigma \equiv \cot \gamma \quad (175)$$

they read

$$f_0(\sigma, \tau) = \frac{1 + \tau^2}{(\sigma + \tau)^2} = \frac{|\lambda_t|^2}{|\lambda_c|^2} \quad (176)$$

$$f_1(\sigma, \tau) = \frac{\sigma\tau - 1}{(\sigma + \tau)^2} = \frac{\operatorname{Re} \lambda_t^* \lambda_u}{|\lambda_c|^2} \quad (177)$$

$$f_2(\sigma, \tau) = \frac{1 + \sigma^2}{(\sigma + \tau)^2} = \frac{|\lambda_u|^2}{|\lambda_c|^2} \quad (178)$$

In the region of interest for a Standard Model test,

$$\sigma = 0.447 \pm 0.253, \quad \tau = 2.54 \pm 0.13 \quad (179)$$

there is a clear hierarchy among the CKM factors

$$f_0 = 0.835_{-0.125}^{+0.162}, \quad f_1/f_0 = 0.018 \pm 0.086, \quad f_2/f_0 = 0.161_{-0.026}^{+0.042} \quad (180)$$

implying $|f_1| \ll f_0$ and $f_2 \ll f_0$. The second inequality is a consequence of the fact that numerically $|V_{ub}/V_{td}|^2 \ll 1$. The first inequality arises because $f_1 \sim \cos \alpha$ and the angle α is close to 90° . A similar feature holds for the decay $B \rightarrow \rho\gamma$, where it leads to a suppression of hadronic uncertainties [52,53]. The dominance of the f_0 term in (173) is re-inforced by the hadronic factors since the difference $|\Delta(K^*)|$ is systematically smaller than $|a_c(K^*)|$. This difference is a next-to-leading order effect in QCD factorization, whereas a_c is present at leading order. In addition, several terms cancel in the difference $a_c - a_u$. First, the NLO hard spectator corrections are identical in the c - and u -sector and drop out, which eliminates the uncertainty due to λ_B . Spectator effects in $a_c - a_u$ can only come from penguin diagrams at NNLO ($\mathcal{O}(\alpha_s^2)$), which are very small [54]. Second, also weak annihilation effects cancel in general, in particular those that are taken into account in our model estimate (coefficients b_i). The only exception would be more complicated $b\bar{d} \rightarrow s\bar{d}d\bar{s}$ annihilation topologies involving charm and up-quark

loops. These are both power and Zweig rule suppressed and not expected to give a significant contribution. Numerically we find

$$|a_c(K^*) - a_u(K^*)|/\text{GeV}^3 = 0.021_{-0.003}^{+0.003} (A_0) \quad -_{+0.004}^{0.003} (\alpha_2^V) \quad +_{-0.006}^{0.006} (m_c) \quad -_{+0.007}^{0.004} (\mu) \quad (181)$$

Normalized to the central value of $|a_c(K^*)| = 0.084$ we then have

$$\frac{|a_c(K^*) - a_u(K^*)|}{|a_c(K^*)|} = 0.25_{-0.10}^{+0.12} \quad (182)$$

Together with the CKM factors from (180) we estimate a relative suppression of the third term in (173) by 0.010 (+0.012, -0.007) with respect to the first term. For the second term we estimate a relative size of at most 0.009 ± 0.043 , neglecting the phase between a_c and Δ . In this case the potential magnitude of the correction depends strongly on the CKM suppression due to f_1 , which can be checked after the CKM factors have been determined at the end of the analysis.

Because of the smallness of the f_1, f_2 terms, the first term in (173) determines the branching fraction to very good approximation. In the $SU(3)$ limit, and up to negligible corrections from electroweak penguins, $a_c(K^*)$ is equal to the penguin amplitude $a_c(\rho)$ in $\bar{B} \rightarrow \rho_L^+ \rho_L^-$ (in a corresponding normalization). Introducing the $SU(3)$ factor

$$|\xi| = \left| \frac{a_c(K^*)}{a_c(\rho)} \right| \approx 1.28 \quad (183)$$

we obtain the ratio of CP averaged branching fractions

$$\frac{B(\bar{B}_d \rightarrow \bar{K}_L^{*0} K_L^{*0})}{B(\bar{B} \rightarrow \rho_L^+ \rho_L^-)} = \frac{((1 - \bar{\rho})^2 + \bar{\eta}^2) |\xi|^2 r_\rho^2}{\bar{\rho}^2 + \bar{\eta}^2 + r_\rho^2 + 2\bar{\rho} r_\rho \cos \phi_\rho} \quad (184)$$

This result constrains the penguin parameter r_ρ in $\bar{B}_d \rightarrow \rho_L^+ \rho_L^-$. The four variables $\bar{\rho}, \bar{\eta}, r_\rho$ and ϕ_ρ may now be determined from the four measurements of $\tau = (1 - \bar{\rho})/\bar{\eta}$, $S_\rho(\bar{\rho}, \bar{\eta}, r_\rho, \phi_\rho)$, $C_\rho(\bar{\rho}, \bar{\eta}, r_\rho, \phi_\rho)$ and $b \equiv B(\bar{B}_d \rightarrow \bar{K}_L^{*0} K_L^{*0})/B(\bar{B} \rightarrow \rho_L^+ \rho_L^-)$. This analysis then depends on a single theoretical parameter, the $SU(3)$ factor $|\xi| = 1.28 \pm 0.14$, where we adopt the estimate in (183) and assign a 50% error on the magnitude of $SU(3)$ breaking. The quantity $\xi = a_c(K^*)/a_c(\rho)$ is real to very good approximation, $\xi \approx |\xi|$.

The expressions for S and C in terms of $\bar{\rho}, \bar{\eta}, r$ and ϕ are identical to the case of $\bar{B}_d \rightarrow \pi^+ \pi^-$ discussed in [19,20]. They read

$$S = \frac{2\bar{\eta}[\bar{\rho}^2 + \bar{\eta}^2 - r^2 - \bar{\rho}(1 - r^2) + (\bar{\rho}^2 + \bar{\eta}^2 - 1)r \cos \phi]}{((1 - \bar{\rho})^2 + \bar{\eta}^2)(\bar{\rho}^2 + \bar{\eta}^2 + r^2 + 2r\bar{\rho} \cos \phi)} \quad (185)$$

$$C = \frac{2r\bar{\eta} \sin \phi}{\bar{\rho}^2 + \bar{\eta}^2 + r^2 + 2r\bar{\rho} \cos \phi} \quad (186)$$

We remark that discrete ambiguities in the determination of $\bar{\rho}, \bar{\eta}, r$ and ϕ can be avoided using other constraints on the unitarity triangle, which exclude $\bar{\rho}, \bar{\eta}$ far outside the region

allowed in the Standard Model [19,20]. A discrete ambiguity in the sign of $\cos\phi_\rho$ can be resolved by the heavy-quark limit, which favours the solution with $\cos\phi_\rho > 0$. As pointed out in a similar context in [51], the discrete choice is still less restrictive in practice, because the second solution has $\cos\phi_\rho < -0.8$, which is in fact far smaller than zero.

The result of this analysis is given in Table 10, where we have also summarized the experimental input from Table 1 and section 5.4. The output values $\bar{\rho}$, $\bar{\eta}$, r_ρ and ϕ_ρ are

Table 10: CKM and penguin parameters extracted from $\tau = \cot\beta = 2.54 \pm 0.13$, $S_\rho = -0.05 \pm 0.17$, $C_\rho = -0.06 \pm 0.13$ and $b = B(\bar{B}_d \rightarrow \bar{K}_L^{*0} K_L^{*0})/B(\bar{B} \rightarrow \rho_L^+ \rho_L^-) = 0.043 \pm 0.015$. The $SU(3)$ breaking parameter is taken to be $|\xi| = 1.28 \pm 0.14$.

	central	τ	S_ρ	C_ρ	b	$ \xi $
$\bar{\rho}$	0.088	-0.010 $+0.011$	-0.029 $+0.029$	-0.000 $+0.010$	-0.009 $+0.011$	$+0.006$ -0.007
$\bar{\eta}$	0.359	-0.014 $+0.015$	$+0.011$ -0.011	$+0.000$ -0.004	$+0.004$ -0.004	-0.002 $+0.003$
$\gamma[\text{deg}]$	76.2	$+1.0$ -1.0	$+4.7$ -4.9	$+0.0$ -1.6	$+1.5$ -1.8	-0.9 $+1.1$
r_ρ	0.064	-0.003 $+0.004$	-0.002 $+0.003$	$+0.000$ -0.000	$+0.010$ -0.012	-0.006 $+0.008$
ϕ_ρ	-0.20	$+0.00$ -0.00	$+0.00$ -0.00	$+0.43$ -0.47	$+0.03$ -0.05	-0.02 $+0.02$

shown together with their sensitivity to the relevant input quantities. From Table 10 we draw the following conclusions:

- a) The errors on the CKM quantities $\bar{\rho}$, $\bar{\eta}$ and γ are rather small. They are dominated by the uncertainty in S_ρ ($\bar{\eta}$ is sensitive also to $\tau = \cot\beta$).
- b) The error from the $SU(3)$ factor $|\xi|$ is smaller than the errors from the experimental quantities τ , S_ρ , b , which may still be improved by future measurements.
- c) The penguin parameter is obtained as $r_\rho = 0.064 \pm 0.014$. The central value is somewhat larger than the theoretical number in (135), but both results are compatible within errors. This confirms the expected smallness of r_ρ , which is the basis for a precise extraction of CKM quantities.
- d) The phase ϕ_ρ is seen to be strongly dependent on C_ρ , but essentially uncorrelated with the remaining parameters and input quantities. In particular $\bar{\rho}$, $\bar{\eta}$ and γ are almost unaffected by the value of C_ρ within the measured range. This behaviour is in agreement with the general expectation discussed in 5.4. The error on ϕ_ρ is completely dominated by the error on C_ρ . The sign of ϕ_ρ is opposite to the central standard model value from factorization in (136). If higher-order perturbative corrections cannot account for this change in sign, and we assume it is not due to

New Physics, this would mean that power corrections give an important contribution to the strong phase. A similar situation is known to occur for the direct CP asymmetries in $\bar{B}_d \rightarrow \pi^+\pi^-$ and $\bar{B}_d \rightarrow \pi^+K^-$. However, within uncertainties the numbers for ϕ_ρ in (136) and Table 10 are fully consistent with each other. The result for ϕ_ρ in Table 10 confirms the prediction of a suppressed phase in the heavy quark limit.

Combining the errors in Table 10 we find for the CKM angles

$$\gamma = (76.2 \pm 5.3)^\circ \quad \alpha = \pi - \beta - \gamma = (82.3 \pm 5.4)^\circ \quad (187)$$

where the uncertainty is dominated by the experimental error in S_ρ . The result is in very good agreement with (143). It is already rather accurate at present. From Table 10 we see that a precision of $\pm 1^\circ$ for γ and α from this method should be possible.

Finally, we remark that the approximations leading to (184) may be cross-checked using the extracted value of γ or $\sigma = \cot \gamma = 0.25 \pm 0.10$, and $\tau = \cot \beta = 2.54 \pm 0.13$. Varying also the hadronic input parameters, the relative importance of the correction terms in (173) is then smaller than $\pm 3\%$. (For the default parameter set and $\sigma = 0.25$, $\tau = 2.54$, the correction is -0.8% .) The corresponding change in (184) could be absorbed in a modification of $|\xi|$ by less than $\pm 1.5\%$, which is entirely negligible.

5.7 Unitarity triangle from $B_d \rightarrow \pi^+\pi^-$ and $B_d \rightarrow \bar{K}^0 K^0$

The analysis of section 5.6 made use of CP violation in $\bar{B}_d \rightarrow \rho_L^+\rho_L^-$, a measurement of $\sin 2\beta$, and the $\bar{B}_d \rightarrow \bar{K}_L^{*0}K_L^{*0}$ branching fraction to obtain an accurate determination of the unitarity triangle. The decay $\bar{B}_d \rightarrow \bar{K}_L^{*0}K_L^{*0}$ served to fix the penguin-to-tree ratio in $\bar{B}_d \rightarrow \rho_L^+\rho_L^-$ based on $SU(3)$ flavour symmetry.

The same analysis may also be performed with the VV -modes replaced by their pseudoscalar counterparts, that is, using CP violation in $\bar{B}_d \rightarrow \pi^+\pi^-$ and constraining the penguin parameter r_π with $\bar{B}_d \rightarrow \bar{K}^0 K^0$ and $SU(3)$ symmetry. The formulas of section 5.6 apply with obvious substitutions. Related discussions can be found in [19,20].

Using form factor estimates based on [55]

$$f_+^{B \rightarrow \pi}(0) = 0.258 \pm 0.031 \quad f_+^{B \rightarrow K}(0) = 0.304 \pm 0.042 \quad (188)$$

we find from QCD factorization [6,23]

$$|\zeta| \equiv \left| \frac{a_c(K)}{a_c(\pi)} \right| = 1.46 \pm 0.23 \quad (189)$$

Again we have assigned a generous 50% uncertainty on the total amount of $SU(3)$ breaking. With experimental input from [24] we obtain the results displayed in Table 11.

Combining errors we obtain from Table 11

$$\gamma = (61.1 \pm 6.8)^\circ \quad (190)$$

Table 11: CKM and penguin parameters extracted from $\tau = \cot \beta = 2.54 \pm 0.13$, $S_\pi = -0.61 \pm 0.08$, $C_\pi = -0.38 \pm 0.07$ and $b \equiv B(\bar{B}_d \rightarrow \bar{K}^0 K^0)/B(\bar{B} \rightarrow \pi^+ \pi^-) = 0.186 \pm 0.040$. The $SU(3)$ breaking parameter is taken to be $|\zeta| = 1.46 \pm 0.23$.

	central	τ	S_π	C_π	b	$ \zeta $
$\bar{\rho}$	0.179	-0.013 $+0.014$	-0.020 $+0.023$	-0.014 $+0.021$	-0.015 $+0.019$	$+0.023$ -0.027
$\bar{\eta}$	0.323	-0.011 $+0.011$	$+0.008$ -0.009	$+0.005$ -0.008	$+0.006$ -0.007	-0.009 $+0.011$
$\gamma[\text{deg}]$	61.1	$+1.0$ -1.0	$+3.3$ -3.7	$+2.3$ -3.4	$+2.5$ -3.1	-3.7 $+4.4$
r_π	0.146	-0.008 $+0.009$	-0.006 $+0.008$	-0.002 $+0.002$	$+0.015$ -0.017	-0.020 $+0.027$
ϕ_π	-0.88	$+0.01$ -0.01	$+0.02$ -0.03	$+0.19$ -0.24	$+0.09$ -0.13	-0.17 $+0.14$

This value is lower than the result in (187) but it remains consistent at the level of roughly 2σ . One possible source of this discrepancy is the rather large value of $C_\pi = -0.38 \pm 0.07$, representing the simple average of the BaBar [56] and Belle [57] results

$$C_\pi = -0.21 \pm 0.09 \quad (\text{BaBar}) \quad C_\pi = -0.55 \pm 0.09 \quad (\text{Belle}) \quad (191)$$

These results are not in very good agreement. With a smaller $|C_\pi|$, favoured by QCD factorization and the BaBar measurement, the extracted value for γ would increase somewhat. For example, with $C_\pi = -0.1$ we obtain $\gamma = 66.6^\circ$, keeping all other inputs fixed. Particularly important for the resulting γ is the value of S_π . If it were 2σ lower in absolute magnitude, at $S_\pi = -0.45$, the central value of γ would shift to $\gamma = 67.4^\circ$. The uncertainties in b and $|\zeta|$ also have a relatively large impact. This is because of the larger size of the penguin contribution r_π in comparison with r_ρ . Note that the error on γ from the uncertainty in b is almost twice as large in Table 11 than in Table 10, even though b is known with an accuracy of 22% in the former case and only to 35% in the latter. Thus, because of the larger size of the penguin amplitude, and also because of the experimental situation of C_π , which is still not entirely resolved, the determination of the unitarity triangle from $\bar{B} \rightarrow \pi^+ \pi^-$ and $\bar{B} \rightarrow \bar{K}^0 K^0$ appears to be somewhat less precise than the determination from $\bar{B} \rightarrow \rho_L^+ \rho_L^-$ and $\bar{B} \rightarrow \bar{K}_L^{*0} K_L^{*0}$.

5.8 CP violation in $B_s \rightarrow \phi_L \phi_L$

The decay $\bar{B}_s \rightarrow \phi\phi$ is a pure $b \rightarrow s$ penguin transition and thus of considerable interest as a New Physics probe. Possible hints of deviations from the Standard Model in CP violation in the $b \rightarrow s$ penguin process $\bar{B}_d \rightarrow \phi K_S$, and similar modes, have so far remained inconclusive. A detailed experimental study of $\bar{B}_s \rightarrow \phi\phi$ will become possible with the LHC [1]. In the Standard Model CP violation in $\bar{B}_s \rightarrow \phi\phi$ is small. Any nonzero effect in excess of the Standard Model contribution will signal the presence of New Physics. Based on our next-to-leading order results we shall investigate the size

and uncertainty of CP violation in the Standard Model, which ultimately limits the sensitivity to New Physics.

The time dependent CP asymmetry in $\bar{B}_s \rightarrow \phi_L \phi_L$ decays is defined by

$$\mathcal{A}_{CP,\phi}(t) = \frac{\Gamma(\bar{B}_s(t) \rightarrow \phi_L \phi_L) - \Gamma(B_s(t) \rightarrow \phi_L \phi_L)}{\Gamma(\bar{B}_s(t) \rightarrow \phi_L \phi_L) + \Gamma(B_s(t) \rightarrow \phi_L \phi_L)} = S_\phi \sin(\Delta m_s t) - C_\phi \cos(\Delta m_s t) \quad (192)$$

Here we have neglected the effects of a nonzero width difference $\Delta\Gamma_{B_s}$, which would modify the time dependence of the CP asymmetry. This can be taken into account in extracting S_ϕ and C_ϕ , but would not change the following discussion of these parameters.

For a generic B decay into a CP self-conjugate final state f one has

$$S = \frac{2 \operatorname{Im}\xi}{1 + |\xi|^2}, \quad C = \frac{1 - |\xi|^2}{1 + |\xi|^2}, \quad \xi = -\frac{M_{12}^*}{|M_{12}|} \frac{A(\bar{B} \rightarrow f)}{A(B \rightarrow f)} \quad (193)$$

where $M_{12} = \langle B | \mathcal{H}_{\Delta B=2} | \bar{B} \rangle$ is the B - \bar{B} mixing amplitude. We use the phase convention $CP|\bar{B}\rangle = -|B\rangle$. The CP violation parameters S_ϕ and C_ϕ then become

$$S_\phi = 2\lambda^2 \eta \operatorname{Re} \frac{a_c(\phi) - a_u(\phi)}{a_c(\phi)}, \quad C_\phi = 2\lambda^2 \eta \operatorname{Im} \frac{a_c(\phi) - a_u(\phi)}{a_c(\phi)} \quad (194)$$

where $a_p(\phi)$, $p = u, c$, is the coefficient of $(iG_F/\sqrt{2})\lambda'_p$ in the $\bar{B}_s \rightarrow \phi_L \phi_L$ amplitude (74) and (113). It can be seen from (194) that S_ϕ and C_ϕ depend on the same CKM quantity but on different hadronic parameters. A measurement of C_ϕ is therefore only of limited use in controlling hadronic uncertainties in S_ϕ .

The hadronic parameters in (194) depend on the difference between the penguin amplitudes from the charm and the up-quark sector. This difference is calculable in factorization. It has the further advantage that the leading annihilation corrections related to the parameters b_i (113) cancel in $a_c(\phi) - a_u(\phi)$. A similar cancellation occurs for the hard-spectator scattering contributions in the NLO approximation. We then find

$$|a_c(\phi) - a_u(\phi)|/\operatorname{GeV}^3 = 0.057_{-0.007}^{+0.007} (A_0) \quad {}_{+0.010}^{-0.008} (\alpha_2^V) \quad {}_{-0.015}^{+0.016} (m_c) \quad {}_{+0.021}^{-0.012} (\mu) \quad (195)$$

where we show the dominant parametric uncertainties and their origin (in brackets). In contrast to the difference $a_c(\phi) - a_u(\phi)$, the absolute value of $a_c(\phi)$ depends on the annihilation contributions b_i . Rather than aiming for an accurate theoretical prediction, it therefore appears more reliable to extract $|a_c(\phi)|$ from experiment. Neglecting the very small up-quark contribution, we may write

$$B(\bar{B}_s \rightarrow \phi_L \phi_L) = \frac{\tau_{B_s} G_F^2 |\lambda'_c|^2}{64\pi m_{B_s}} |a_c(\phi)|^2 \quad (196)$$

This gives

$$|a_c(\phi)| = 0.177 \operatorname{GeV}^3 \left[\frac{B(\bar{B}_s \rightarrow \phi_L \phi_L)}{15 \cdot 10^{-6}} \right]^{1/2} \left[\frac{1.53 \operatorname{ps}}{\tau_{B_s}} \right]^{1/2} \quad (197)$$

First evidence for the decay $\bar{B}_s \rightarrow \phi\phi$ has been reported by the CDF collaboration, which quotes [58]

$$B(\bar{B}_s \rightarrow \phi\phi) = (14_{-5}^{+6}(\text{stat}) \pm 6(\text{syst})) \cdot 10^{-6} \quad (198)$$

This is not yet the longitudinal branching fraction needed in (197), and the error is still large. By the time CP violation in $\bar{B}_s \rightarrow \phi\phi$ will be studied at the LHC, the branching fraction will be known with good precision and the number in (197) can be easily updated.

The quantity S_ϕ is predicted to be small and positive in the Standard Model. With our default parameter set and $\eta = 0.36$ we obtain

$$S_\phi(\text{default}) \approx 0.01 \quad (199)$$

From the discussion above we conclude that the Standard Model upper limit can be written as

$$S_\phi \lesssim 2\lambda^2\eta \frac{|a_c(\phi) - a_u(\phi)|}{|a_c(\phi)|} \lesssim \lambda^2\eta \left[\frac{B(\bar{B}_s \rightarrow \phi_L\phi_L)}{15 \cdot 10^{-6}} \right]^{-1/2} \quad (200)$$

A similar limit holds for the absolute value of C_ϕ . For $\eta \lesssim 0.4$ we have

$$S_\phi \lesssim 0.02 \quad |C_\phi| \lesssim 0.02 \quad (201)$$

A rescaling for the actual value of the branching fraction, which might deviate from the assumed default value of $15 \cdot 10^{-6}$, can be done using (200). Measurements in excess of these Standard Model limits would constitute evidence for New Physics. The expected sensitivity of LHCb after five years of data taking is $\sigma(S_\phi) \approx 0.05$ [59]. Improvements to values of 0.01 or 0.02 with the anticipated LHCb upgrade appear possible [1]. This should allow us to exploit the full New Physics potential of S_ϕ and to detect non-standard effects in $b \rightarrow s$ penguins at the few percent level.

6 Comparison with the literature

In this section we comment briefly on the existing literature related to the subject of the present paper [9–18].

We re-emphasize that factorization calculations for charmless two-body B decays, in particular $B \rightarrow V_L V_L$, are useful for flavour physics analyses such as the determination of CKM parameters. This has also been stressed in [11] and earlier in [6,19,20,23]. The most comprehensive study of $B \rightarrow VV$ decays has been presented in [11] with an emphasis on total branching fractions and polarization observables, for instance the longitudinal polarization fractions f_L . More recently these processes were considered in [18] in an extended study, following the analysis of [11]. We do not discuss transverse polarization here but rather concentrate on the decays with longitudinal vector mesons $B \rightarrow V_L V_L$. These are calculable in QCD in the heavy-quark limit and thus of special interest for phenomenological applications in flavour physics. We list the detailed results

for the $B \rightarrow V_L V_L$ amplitudes in explicit terms. The corresponding results of [11] can be reconstructed from similar formulas given for $B \rightarrow PV$ decays in [23]. Our main results are consistent with [11]. A minor difference with (the original version of) [11] are the expressions for penguin annihilation $A_3^i \approx 0$ and A_3^f (84). The final expressions in [11] give incorrectly, due to a relative sign change, a nonvanishing A_3^i and $A_3^f \approx 0$, even though the basic formulas agree with (82). The difference leads to a reduced sensitivity to penguin annihilation in penguin-dominated $B \rightarrow V_L V_L$ decays. It does not play a role for $\bar{B} \rightarrow \rho^+ \rho^-$, because the corresponding decay amplitude is tree dominated and color allowed, so no deviations from modelling of power-suppressed contributions are expected. This point has previously been noted in [18]. There is consensus on the expressions (82), (84) within the annihilation model used [9,18,61]. Another difference with [11,23] is the treatment of electromagnetic penguin matrix elements contributing to $a_{7,9}^u$, where we have proposed an explicit model for the long-distance contributions to these $\mathcal{O}(\alpha)$ terms.

The article [9] concentrates on transverse polarization and therefore does not report the complete expressions for the amplitudes with longitudinal vector mesons. Where a comparison is possible we agree with the results of [9], except for two minor discrepancies. One is the detailed form of the integrand of the annihilation parameter A_3^f . However, the final result for A_3^f coincides with ours. Another difference is the annihilation part of $B^- \rightarrow K^{*-} \phi$, which should read $b_3 + b_3^{\text{EW}}$ instead of $b_3 - b_3^{\text{EW}}/2$. Both issues are inconsequential.

$B \rightarrow VV$ decays have been studied within QCD factorization also in [13–18]. These papers address various VV channels, especially penguin dominated modes such as ϕK^* . Some of them investigate the impact of New Physics scenarios [15,16,17], [18] extends the analysis to VA and AA modes as well. In comparison, the present paper, while concentrating on $B \rightarrow V_L V_L$, gives complete NLO results for all channels, a detailed analysis of uncertainties and applications for precision tests of flavour physics. The authors of [18] employ $m_c(m_b) = 0.91$ GeV, smaller than the value used here and in [11]. We find that the error due to m_c for the longitudinal amplitude is small compared to other experimental input, also for penguin dominated decays.

7 Conclusions

In this paper we presented a systematic analysis of B -meson decays into a pair of longitudinal vector mesons. The main results can be summarized as follows:

- Explicit formulas are given for the complete set of $\Delta S = 0$ and $\Delta S = 1$ decay amplitudes of $\bar{B} \rightarrow V_L V_L$ at NLO in QCD factorization. Estimates of power corrections from weak annihilation are included to study the sensitivity to effects of this kind in phenomenological applications. The set of decays considered comprises 17 $\Delta S = 0$ and 17 $\Delta S = 1$ channels, including 2 and 4 pure annihilation modes, respectively.

- The agreement with the available measured branching ratios of \bar{B}_d , B^- decays into $\rho^+\rho^-$, $\rho^0\rho^0$, $\rho^-\rho^0$, $\bar{K}^{*0}K^{*0}$, $\bar{K}^{*0}\rho^0$, $K^{*-}\rho^+$, $K^{*-}\rho^0$, $\bar{K}^{*0}\rho^-$, $\bar{K}^{*0}\phi$, $K^{*-}\phi$ and $\bar{K}^{*0}\omega$ is very good, within current uncertainties and with the central values used for $\bar{B} \rightarrow V_L$ form factors. The decay to $\rho^-\omega$ agrees at the level of about 2σ . We note that QCD factorization works well in particular for the penguin modes and for the three $\rho\rho$ channels and their characteristic hierarchy of branching fractions. Our hadronic input is based on the available literature. No tuning of parameters has been done to improve the fit with data.
- Long-distance electromagnetic penguins in B decays with neutral vector mesons ρ^0 , ω or ϕ are taken into account using a model description. They are of some conceptual interest but their numerical impact is generally small.
- The deviation from ideal mixing in the ω - ϕ system is found to have a small effect on most decay modes with these particles in the final state. The impact is very large for $B^- \rightarrow \rho^-\phi$.
- We advocate the direct use of mixing-induced CP violation in $\bar{B}_d \rightarrow \rho_L^+\rho_L^-$, measured by S_ρ , to extract the parameters of the unitarity triangle. Together with $\sin 2\beta$ the current measurements of S_ρ imply (143)

$$\gamma = (72.4 \pm 6.2)^\circ \quad (202)$$

where the error is dominated by S_ρ . This analysis benefits from the small penguin-to-tree ratio for vector modes $r_\rho = 0.038 \pm 0.024$ (135), which leads to a residual theory uncertainty in γ of $\pm 3^\circ$.

- We propose a method to relate the penguin contribution in $\bar{B}_d \rightarrow \rho_L^+\rho_L^-$ to the decay $\bar{B}_d \rightarrow \bar{K}_L^{*0}K_L^{*0}$ based on the V -spin subgroup of flavour $SU(3)$. This makes it possible to constrain the uncertainties due to penguin power corrections, especially from annihilation topologies, and provides us with a check on the penguin-to-tree ratio calculated in QCD factorization. The absolute value determined by the V -spin method, $r_\rho = 0.064 \pm 0.014$, is consistent with the calculation in QCD factorization. The resulting angle

$$\gamma = (76.2 \pm 5.3)^\circ \quad (203)$$

has a residual theory error of $\pm 1^\circ$.

- A comparison of the analyses mentioned in the previous two items to the corresponding ones with pseudoscalar decay modes suggests that the hadronic uncertainties are better under control in the case of vector modes.
- We point out that within the SM $\sin 2\beta$ and the CP violation parameter S_ρ in $\bar{B} \rightarrow \rho_L^+\rho_L^-$ determine

$$|V_{ub}| = (3.54 \pm 0.17) \cdot 10^{-3} \quad (204)$$

where the error is at present still entirely dominated by $\sin 2\beta$. Hadronic uncertainties enter only at second order in S_ρ and the penguin parameter r_ρ and are below 2%. Possible New Physics affecting the $B_d - \bar{B}_d$ mixing phase can be constrained by comparing the above value of $|V_{ub}|$ with direct determinations from exclusive or inclusive $b \rightarrow ul\nu$ decays.

- In future measurements $\bar{B}_s \rightarrow \phi\phi$ will provide tests for New Physics. We present a bound on S_ϕ and C_ϕ , which will further improve when more data are available.

The phenomenology of $\bar{B} \rightarrow V_L V_L$ decays is rich and promising. QCD factorization provides a solid theoretical basis for these processes. With the measurement of additional channels and improved precision for the ones already observed, many more applications in flavour physics may be foreseen.

A Long-distance electromagnetic penguins

For B decays with neutral vector mesons ρ^0 , ω or ϕ , the operators $Q_{1,2}^p$ have electromagnetic penguin-type matrix elements where the photon from the $p\bar{p}$ loop is transformed into one of these mesons. The photon virtuality $k^2 = m_V^2$ is then small. While the penguin loop may still be considered short-distance dominated for $p = c$ due to the charm-quark mass, the matrix element becomes sensitive to long-distance hadronic physics for $p = u$. This can be seen from the perturbative result for the case of the charm quark (38), which diverges in the limit $m_c \rightarrow 0$. The up-quark contribution is thus not strictly calculable. Since this situation arises only in a small electromagnetic correction, it is not a serious problem for practical purposes. In fact, additional dependence on long-distance hadronic physics is to be expected when electromagnetic radiative corrections to hadronic B decays are considered. Still the penguin matrix element under discussion contributes within our approximation scheme of including leading electroweak effects. We shall therefore give an estimate of its size using available information on the long-distance dynamics of the up-quark loop. Apart from obtaining a numerical evaluation of the effect, the long-distance electromagnetic penguin is also interesting for conceptual reasons.

The up-quark loop is closely related to the vacuum polarization function $\Pi(k^2)$, where the UV subtraction is given by the standard renormalization prescription of the weak hamiltonian. We thus write the penguin matrix element, needed at low photon virtuality $k^2 = m_V^2$, as the matrix element evaluated at $k^2 = m_b^2$ plus a remainder proportional to the difference $\Pi(k^2) - \Pi(m_b^2)$. The contribution of the electromagnetic up-quark penguin to the coefficients $a_{7,9}^u$ then takes the form

$$\Delta a_{7,9}^u = \frac{\alpha}{9\pi} (C_1 + N_c C_2) \left[\frac{4}{3} \ln \frac{m_b}{\mu} - \frac{4}{9} - \frac{2\pi}{3} i - \frac{8\pi^2}{N_c} (\Pi(m_V^2) - \Pi(m_b^2)) \right] \quad (205)$$

The correlator $\Pi(k^2)$ is defined through

$$\Pi_{\mu\nu}(k) = i \int d^4x e^{ik \cdot x} \langle 0 | T j_\mu(x) j_\nu(0) | 0 \rangle \equiv (k_\mu k_\nu - k^2 g_{\mu\nu}) \Pi(k^2) \quad (206)$$

where $j_\mu = \bar{u}\gamma_\mu u$. The first terms in the square brackets of (205) come from the perturbative evaluation of the matrix element at $k^2 = m_b^2$ and carry the appropriate scale and scheme dependence. The remainder depending on Π may be computed to lowest (one-loop) order, which reproduces the perturbative result for the matrix element. We shall treat $\Pi(k^2) - \Pi(m_b^2)$ as the full hadronic correlator, which includes the nonperturbative hadronic physics relevant at low k^2 . This procedure assumes a factorization of the soft hadronic correlator from the remaining parts of the diagram, which is not strictly justified. We adopt this additional assumption to obtain a rough estimate of the long-distance sensitive penguin contribution. A similar method has been proposed and applied in the context of $b \rightarrow s(d)e^+e^-$ decays in [60].

The function $\Pi(k^2)$ obeys the dispersion relation

$$\Pi(k^2) = \frac{1}{\pi} \int_0^\infty dt \frac{\text{Im}\Pi(t)}{t - k^2 - i\epsilon} \quad (207)$$

In this form the dispersion relation needs one subtraction, but the subtraction constant cancels in $\Pi(k^2) - \Pi(m_b^2)$. In principle $\text{Im}\Pi(t)$ could be determined experimentally. Instead, for simplicity, we choose a convenient ansatz that should capture the essential features of the true hadronic quantity $\text{Im}\Pi(t)$. We write $\text{Im}\Pi$ as the sum of a resonance and a continuum contribution

$$\text{Im}\Pi = \text{Im}\Pi_r + \text{Im}\Pi_c \quad (208)$$

where

$$\text{Im}\Pi_r(t) = \sum_{r=\rho,\omega} \frac{1}{2} \frac{f_r^2 m_r \Gamma_r}{(t - m_r^2)^2 + m_r^2 \Gamma_r^2} \quad (209)$$

$$\text{Im}\Pi_c(t) = \frac{t}{4\pi t_c} \Theta(t_c - t) + \frac{1}{4\pi} \Theta(t - t_c), \quad t_c = 4\pi^2(f_\rho^2 + f_\omega^2), \quad t > 0 \quad (210)$$

The asymptotic QCD result fixes $\text{Im}\Pi_c$ to $N_c/(12\pi) = 1/(4\pi)$ at large t . Imposing quark-hadron duality for the integral of $\text{Im}\Pi(t)$ up to (at least) $t = t_c$ determines the value of $t_c = 4\pi^2(f_\rho^2 + f_\omega^2) \approx 3.1 \text{ GeV}^2$. The factor 1/2 in (209) is an isospin factor coming from the overlap of ρ^0 and ω with the $\bar{u}\gamma_\mu u$ current. Determining Π in (205) with the help of (207) and (208), treating the resonances as narrow and taking the heavy-quark limit $t_c \ll m_b$, we finally obtain (39). Concerning the factor in square brackets in (39), two limiting cases are worth noting. If $k^2 = m_V^2 \rightarrow 0$, we recover an expression similar to (38) where the light-quark mass under the logarithm is replaced by the hadronic scale $\sqrt{t_c}$. In the limit $k^2 = m_V^2 \rightarrow t_c$ the same terms appear, and in addition the perturbative imaginary part $-2\pi i/3$.

B Coefficients a_i, b_i

In the following Table we quote the central values of the coefficients a_i as defined in (23) for two final-state ρ -mesons (3). The default value used for the model of power-

suppressed hard-spectator contributions is $X_H = \ln \frac{m_B}{\Lambda_h}$ and for the renormalization scale it is $\mu = 4.2\text{GeV}$.

a_1	a_2	$a_3 + a_5$	a_4^u	a_4^c
$0.991 + 0.020i$	$0.177 - 0.084i$	$0.002 - 0.001i$	$-0.025 - 0.016i$	$-0.033 - 0.009i$
$(a_7^u + a_9^u)/\alpha$	$(a_7^u - a_9^u)/\alpha$	$(a_7^c + a_9^c)/\alpha$	a_{10}^u/α	a_{10}^c/α
$-1.84 - 0.54i$	$1.15 + 0.02i$	$-1.10 - 0.02i$	$-0.17 + 0.09i$	$-0.17 + 0.09i$

The central values of the coefficients b_i as defined in (78) for two final-state ρ -mesons (3) are given below. The default value used for the model of power-suppressed annihilation contributions is $X_A = \ln \frac{m_B}{\Lambda_h}$ and for the renormalization scale it is $\mu = 4.2\text{GeV}$. Here $r_A = B_{\rho\rho}/A_{\rho\rho}$.

$r_A b_1$	$r_A b_2$	$r_A b_3$	$r_A b_4$	$r_A b_3^{EW}/\alpha$	$r_A b_4^{EW}/\alpha$
0.029	-0.011	0.003	-0.003	-0.035	0.013

Acknowledgements

We thank Martin Beneke and Matthias Neubert for useful discussions. This work was supported in part by the DFG cluster of excellence ‘Origin and Structure of the Universe’ and by the DFG Graduiertenkolleg GK 1054.

References

- [1] M. Artuso *et al.*, arXiv:0801.1833 [hep-ph].
- [2] M. Bona *et al.*, arXiv:0709.0451 [hep-ex].
- [3] T. Kageyama, AIP Conf. Proc. **842** (2006) 1064.
- [4] T. Browder *et al.*, JHEP **0802** (2008) 110 [arXiv:0710.3799 [hep-ph]].
- [5] T. E. Browder, T. Gershon, D. Pirjol, A. Soni and J. Zupan, arXiv:0802.3201 [hep-ph].
- [6] M. Beneke, G. Buchalla, M. Neubert and C. T. Sachrajda, Nucl. Phys. B **606** (2001) 245 [arXiv:hep-ph/0104110].
- [7] M. Beneke, G. Buchalla, M. Neubert and C. T. Sachrajda, Phys. Rev. Lett. **83** (1999) 1914 [arXiv:hep-ph/9905312].
- [8] M. Beneke, G. Buchalla, M. Neubert and C. T. Sachrajda, Nucl. Phys. B **591** (2000) 313 [arXiv:hep-ph/0006124].

- [9] A. L. Kagan, Phys. Lett. B **601** (2004) 151 [arXiv:hep-ph/0405134].
- [10] C. Kraus, Decays of B mesons into two light vector mesons, Diploma Thesis, LMU Munich, 2004
- [11] M. Beneke, J. Rohrer and D. Yang, Nucl. Phys. B **774** (2007) 64 [arXiv:hep-ph/0612290].
- [12] M. Beneke, J. Rohrer and D. Yang, Phys. Rev. Lett. **96** (2006) 141801 [arXiv:hep-ph/0512258].
- [13] H. Y. Cheng and K. C. Yang, Phys. Lett. B **511** (2001) 40 [arXiv:hep-ph/0104090].
- [14] X. Q. Li, G. r. Lu and Y. D. Yang, Phys. Rev. D **68** (2003) 114015 [Erratum-ibid. D **71** (2005) 019902] [arXiv:hep-ph/0309136].
- [15] Y. D. Yang, R. M. Wang and G. R. Lu, Phys. Rev. D **72** (2005) 015009 [arXiv:hep-ph/0411211].
- [16] P. K. Das and K. C. Yang, Phys. Rev. D **71** (2005) 094002 [arXiv:hep-ph/0412313].
- [17] C. S. Huang, P. Ko, X. H. Wu and Y. D. Yang, Phys. Rev. D **73** (2006) 034026 [arXiv:hep-ph/0511129].
- [18] H. Y. Cheng and K. C. Yang, arXiv:0805.0329 [hep-ph].
- [19] G. Buchalla and A. S. Safir, Phys. Rev. Lett. **93** (2004) 021801 [arXiv:hep-ph/0310218].
- [20] G. Buchalla and A. S. Safir, Eur. Phys. J. C **45** (2006) 109 [arXiv:hep-ph/0406016].
- [21] G. Buchalla, A. J. Buras and M. E. Lautenbacher, Rev. Mod. Phys. **68** (1996) 1125 [arXiv:hep-ph/9512380].
- [22] J. Charles, A. Le Yaouanc, L. Oliver, O. Pene and J. C. Raynal, Phys. Rev. D **60** (1999) 014001 [arXiv:hep-ph/9812358].
- [23] M. Beneke and M. Neubert, Nucl. Phys. B **675** (2003) 333 [arXiv:hep-ph/0308039].
- [24] E. Barberio *et al.* [Heavy Flavor Averaging Group (HFAG) Collaboration], arXiv:0704.3575 [hep-ex]; <http://www.slac.stanford.edu/xorg/hfag/>
- [25] B. Aubert *et al.* [BaBar Collaboration], Phys. Rev. Lett. **100** (2008) 081801 [arXiv:0708.2248 [hep-ex]].
- [26] P. Goldenzweig, arXiv:0807.4271 [hep-ex].
- [27] B. Aubert *et al.* [BaBar Collaboration], arXiv:0807.3935 [hep-ex].

- [28] W. M. Yao *et al.* [Particle Data Group], J. Phys. G **33** (2006) 1.
- [29] J. Charles *et al.* [CKMfitter Group], Eur. Phys. J. C **41** (2005) 1 [arXiv:hep-ph/0406184]; <http://ckmfitter.in2p3.fr>
- [30] M. Bona *et al.* [UTfit Collaboration], JHEP **0507** (2005) 028 [arXiv:hep-ph/0501199]; <http://www.utfit.org>
- [31] P. Ball, G. W. Jones and R. Zwicky, Phys. Rev. D **75** (2007) 054004 [arXiv:hep-ph/0612081].
- [32] P. Ball and R. Zwicky, Phys. Rev. D **71** (2005) 014029 [arXiv:hep-ph/0412079].
- [33] P. Ball and G. W. Jones, JHEP **0703** (2007) 069 [arXiv:hep-ph/0702100].
- [34] G. Buchalla, arXiv:0809.0532 [hep-ph].
- [35] M. Gronau and J. L. Rosner, Phys. Lett. B **666** (2008) 185 [arXiv:0806.3584 [hep-ph]].
- [36] B. Aubert *et al.* [Babar Collaboration], Phys. Rev. D **76** (2007) 052007 [arXiv:0705.2157 [hep-ex]].
- [37] K. Abe *et al.* [Belle Collaboration], Phys. Rev. D **76** (2007) 011104 [arXiv:hep-ex/0702009].
- [38] A. J. Buras, M. E. Lautenbacher and G. Ostermaier, Phys. Rev. D **50** (1994) 3433 [arXiv:hep-ph/9403384].
- [39] A. Poluektov *et al.* [Belle Collaboration], Phys. Rev. D **73** (2006) 112009 [arXiv:hep-ex/0604054].
- [40] B. Aubert *et al.* [Babar Collaboration], arXiv:0804.2089 [hep-ex].
- [41] F. J. Botella and J. P. Silva, Phys. Rev. D **70** (2004) 096007 [arXiv:hep-ph/0312337].
- [42] L. Lavoura, Eur. Phys. J. C **40** (2005) 187 [arXiv:hep-ph/0402181].
- [43] M. Neubert, arXiv:0801.0675 [hep-ph].
- [44] C. Bourrely, I. Caprini and L. Lellouch, arXiv:0807.2722 [hep-ph].
- [45] P. Ball, Phys. Lett. B **644** (2007) 38 [arXiv:hep-ph/0611108].
- [46] G. Duplancic, A. Khodjamirian, T. Mannel, B. Melic and N. Offen, JHEP **0804** (2008) 014 [arXiv:0801.1796 [hep-ph]]. .
- [47] V. Lubicz and C. Tarantino, arXiv:0807.4605 [hep-lat].

- [48] Y. Grossman, Y. Nir and M. P. Worah, Phys. Lett. B **407** (1997) 307 [arXiv:hep-ph/9704287].
- [49] R. Fleischer, G. Isidori and J. Matias, JHEP **0305** (2003) 053 [arXiv:hep-ph/0302229].
- [50] B. Aubert *et al.* [BABAR Collaboration], Phys. Rev. Lett. **99** (2007) 231802 [arXiv:0708.1544 [hep-ex]].
- [51] M. Beneke, M. Gronau, J. Rohrer and M. Spranger, Phys. Lett. B **638** (2006) 68 [arXiv:hep-ph/0604005].
- [52] S. W. Bosch and G. Buchalla, JHEP **0501** (2005) 035 [arXiv:hep-ph/0408231].
- [53] M. Beneke, T. Feldmann and D. Seidel, Eur. Phys. J. C **41** (2005) 173 [arXiv:hep-ph/0412400].
- [54] M. Beneke and S. Jäger, Nucl. Phys. B **768** (2007) 51 [arXiv:hep-ph/0610322].
- [55] P. Ball and R. Zwicky, Phys. Rev. D **71** (2005) 014015 [arXiv:hep-ph/0406232].
- [56] B. Aubert *et al.* [BABAR Collaboration], Phys. Rev. Lett. **99** (2007) 021603 [arXiv:hep-ex/0703016].
- [57] H. Ishino *et al.* [Belle Collaboration], Phys. Rev. Lett. **98** (2007) 211801 [arXiv:hep-ex/0608035].
- [58] D. E. Acosta *et al.* [CDF Collaboration], Phys. Rev. Lett. **95** (2005) 031801 [arXiv:hep-ex/0502044].
- [59] S. Amato, B. Souza de Paula, J. McCarron, F. Muheim and Y. Xie, LHCb public note, CERN-LHCB-2007-047
- [60] F. Krüger and L. M. Sehgal, Phys. Lett. B **380** (1996) 199 [arXiv:hep-ph/9603237].
- [61] M. Beneke, private communication.